CHALMERS
UNIVERSITY OF TECHNOLOGY

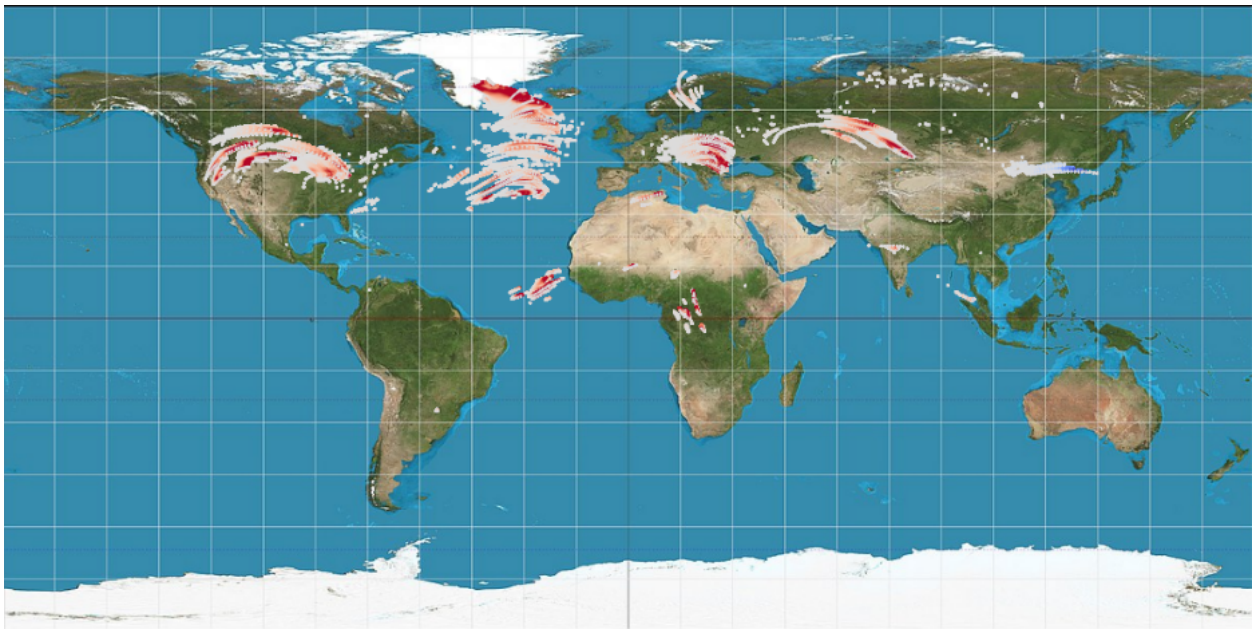

Analyzing the climate impact of contrails with the use of sustainable aviation fuels

Master's thesis in Sustainable Energy Systems

Manuel Marcks

Space, Earth and Environment

CHALMERS UNIVERSITY OF TECHNOLOGY
Gothenburg, Sweden 2024
www.chalmers.se

Master's thesis 2024

Analyzing the climate impact of contrails with the use sustainable aviation fuels

MANUEL MARCKS

CHALMERS
UNIVERSITY OF TECHNOLOGY

Department of Space, Earth and Environment
Physical resource theory
Chalmers University of Technology
Gothenburg, Sweden 2024

Analyzing the climate impact of contrails
with the use of sustainable aviation fuels
MANUEL MARCKS

Supervisor: Susanne Pettersson, Department of Space, Earth and Environment
Examiner: Daniel Johansson, Department of Space, Earth and Environment

Master's Thesis 2024
Department of Space, Earth and Environment
Physical resource theory
Chalmers University of Technology
SE-412 96 Gothenburg
Telephone +46 31 772 1000

Cover: Visualization of the contrails with jet fuel on the first of July between 13:48 and 18:36 with starting point in Europe

Typeset in LaTeX
Printed by Chalmers Reproservice
Gothenburg, Sweden 2024

Analyzing the climate impact of contrails with the use of sustainable aviation fuels

Manuel Marcks
Department of Space, Earth and Environment
Chalmers University of Technology

Abstract

Contrails contribute to climate warming with a phenomenon known as energy forcing, which can be mitigated by employing sustainable aviation fuels (SAF). The European Union aims to incorporate at least 5 % SAF by 2030, but the impact of SAF on energy forcing varies significantly with time and location. To align with the EU's objective, this study focuses solely on flights originating in Europe.

Contrails form when the exhaust gas from an aircraft engine mixes with the surrounding air, which must meet specific conditions such as those defined by the Schmidt-Appleman criterion. This criterion requires that the ambient temperature and humidity levels reach certain thresholds. Under these conditions, the water vapor from the exhaust and the atmosphere condenses and freezes onto the soot particles present in the exhaust gases, leading to the formation of visible contrails.

The objective of this Master's thesis is to develop and assess various strategies for targeted SAF utilization. Thus, the following research question is posed: "What is the optimal strategy for maximizing SAF-induced reduction in energy forcing and what practical guideline can be derived to implement this strategy?"

To address the research question, flight data for July 1^{st}, 2019, was provided. Using a *python* program named "Contrail Cirrus Prediction Model", the climate impact of contrail formation and contrail cirrus can be simulated and analyzed. To consider several days, the flight data was extended by adjusting the date to take different meteorological data into account.

The initial approach involved defining SAF blends ranging from 100 % to 5 % SAF mixed with jet fuel, to be used during the time of day with the highest energy forcing. The duration of SAF usage varied for each blend to achieve a total 5 % SAF utilization daily. Additionally, flights from Europe to North America were considered, utilizing a blend comprising 29.51 % SAF and 70.49 % jet fuel. The same was done with intra-European flights using a blend of 9.63 % SAF and 90.37 % jet fuel.

The greatest reduction in energy forcing was observed when employing SAF in flights from Europe to North America, achieving an average reduction of 14.65 % over six analyzed days. This reduction is relative to the energy forcing caused from all flights originating in Europe. Following this, a blend of 50 % SAF and 50 % jet fuel, used during the two hour 24 minute period with the highest energy forcing, yielded an average reduction of 9.62 %. Subsequent reductions were observed with blends of 100 %, 75 %, 25 % and 5 %. The least reduction occurred when utilizing SAFs for inter-european flights, averaging only 0.38 %.

Furthermore, this thesis aimed to identify the time of day with the highest reduction potential for SAF usage to give a recommendation when to use it. Based on the findings, it is recommended to use SAF in the afternoon during winter and spring,

in the evening during summer, and in the late morning during autumn. However, further analysis of additional days and flights to continents beyond North America is required to optimize SAF utilization recommendations.

Keywords: aviation, climate, contrails, emission, sustainable.

Acknowledgements

First, I would like to express my gratitude to my supervisor, Susanne Petterson, for her continuous support and patience. Our weekly meetings and discussions have been enlightening, and her guidance has been invaluable in navigating through the challenges of this thesis.

My examiner Daniel Johansson provided valuable and helpful comments on my work and his expertise has been instrumental in shaping my research project.

I am grateful for my fellow students for their assistance, feedback and continuous mental support. Their collaborative spirit motivated me throughout this process.

Lastly, I would like to thank my family for their support, understanding, and unwavering belief in me throughout this journey.

Manuel Marcks, Gothenburg, 05 2024

List of Acronyms

Below is the list of acronyms that have been used throughout this thesis listed in alphabetical order:

accf$_{NO_x}$	NO_x induced temperature change per emitted NO_2 emission, accounted for NO_x efficacy effects
CH$_4$	methane
CO	carbon monoxide
CO$_2$	carbon dioxide
CoCiP	contrail cirrus prediction model
ei	emission index
EF	energy forcing
EU	European Union
ERF	effective radiative forcing
HC	hydrocarbon
LW	longwave
NO$_x$	nitrogen oxides
nvPM	non-volatile particulate matter
O$_3$	Ozone
pmo	primary mode ozone
RF	radiative forcing
SAC	Schmidt-Appleman criterion
SAF	sustainable aviation fuel
SW	short wave

Nomenclature

Below is the nomenclature of indices, sets, parameters, and variables that have been used throughout this thesis.

Indices

$blend$	index for blend
ei	emission index
i	ice
m	index for mass
n	index for number
ref	reference
SAF	sustainable aviation fuel
t	index for time step
x	index for a number

Parameters

α_i	coefficient

Variables

EF	effective forcing
$\hat{F}$	thrust settings
H	hydrogencontent
L	length
$nvPM$	non-volatalie particulate matter
p	mixture

RF	radiative forcing
W	width

Contents

List of Figures

List of Tables

1
Introduction

1.1 Climate impact of contrails

Politics, industries, a normal citizen and therefore the whole world are facing the same urgent challenge: reduce and deal with the climate change. 2023 was the warmest year since data recording started with a global average temperature of 1.4 °C higher than preindustrial levels [1]. Considering the goal set by the Paris climate agreement from 2015 to limit the antrophogenic climate change to at least 2 °C until 2050, there is not much time left to get things in order [2]. Everyone and every industry must do his part and so does the global aviation industry, which is addressing the impacts of the climate change while holding up its economic and social significance.

The aviation sector accounts for approximately 5 % of climate warming [3], but compared to other sectors, it is still in its early stages of addressing emission. Sectors like electricity generation, renewable energies such as wind, solar and hydro power are already well established, with increasing growth rates and mature technologies. Similarly the share of electric vehicles continues to grow in the mobility sector. However, in aviation, the majority of aircrafts still rely on traditional fuels, which is most likely kerosene [4]. In 2020 the share of sustainable aviation fuel (SAF) was under 0.05 %. This indicates a lack of significant progress in reducing aviation's impact on climate change, but at the same time shows a high potential and a lot of possibilities. Furthermore, the reliance on fossil fuels makes transitioning to alternative fuels a desirable objective.

The reduction of the climate impact is even more important considering, that predictions suggest that the number of flights will continue to rise in the future. It is estimated that the number of flights could triple by 2050, respectively an annual growth rate of approximately 3.6% to 4.3% [5]. This implies up to a tripling of carbon dioxide (CO_2) emissions but also an increase in contrail formation. Contrails are ice clouds, which can from due to the exhaust of an aircraft. These contrails can also have a high warming climatic impact. While the overall impact will correspondingly rise, certain regions may experience significant local impacts due to the high density of contrails in specific areas. Consequently, considerable research efforts have been directed towards finding alternative propulsion methods for aircraft, with hydrogen and SAF emerging as the most promising options.

The European Union has set ambitious targets to increase the use of SAF in flights departing from European airports. By 2030, the aim is to achieve a 5 % share of SAF, amounting to approximately 2.3 million tonnes [6]. This target is projected

to expand further in subsequent years, with a goal of 32 % by 2040 and 63 % by 2050. Achieving these targets would require significant production of SAF, but it is expected to result in a substantial reduction of approximately 60 % in CO_2 emissions [6].

Moreover, the use of SAF not only mitigates CO_2 emissions, but also has a notable impact on the formation of contrails and their subsequent climate effects. Therefore, increasing the utilization of SAF represents a multifaceted approach to addressing environmental concerns within the aviation industry.

1.2 Aim and limitations of the Thesis

"The Master thesis project aims to investigate the consequences of the inclusion of biofuels in conventional fuel on the properties of contrail cirrus with special focus on changes in energy forcing and to analyze benefits of using SAFs under certain conditions such as time of day" [3]. The primary objective is to find a distribution for a fixed amount of SAFs, which limits the warming effect of contrails as much as possible, since the contrail formation and the effect of these contrails depends strongly on atmospheric conditions and can differ strongly in time and space. This means to find a time of the day or flight paths where use of the same amount of SAFs leads to a greater decrease of the warming effect of the contrails than with an even distribution of SAFs over the whole day. Since the European Union (EU) set the goal to have a share of 5 % of SAF use throughout the year in Europe in 2030 [6], this will be the goal or the amount of SAF what is being worked with. To perform the simulations to investigate the effect of the contrails with and without SAFs a program called *contrail cirrus prediction model (CoCiP)* is used.

The analysis is constrained by the availability of flight data, which, prior to the thesis, was obtained for a single day (2019-07-01) upon request from the corresponding author [7]. Consequently, the investigation is restricted to this specific day, encompassing 24 hours. Additional data did not become accessible during the course of the thesis. Therefore, the provided data was adjusted by changing the date to be able to run the model with different meteorological data. Notably, the modeling approach solely utilizes historical flight paths and does not involve future prediction models. Moreover, the flight paths remain fixed throughout the study and are not subject to alteration. The focus of the study will be the flights with their starting airport in Europe.

The central research inquiry revolves around determining the degree of influence exerted by varying for example the operational timing of SAFs or the flight paths, where the SAFs are used. This entails fixing the quantity of SAFs used while altering the time of day during which they are employed. Additionally, the influence of SAF-use in certain flight routes will be investigated. Also the seasonal influence will be taken into account. Emphasis is placed on evaluating the efficacy of utilizing SAFs within a specified quantity. As a conclusion, an optimal time window or flight path for SAF utilization will be identified to maximize its impact.

2
Theory

To create the models, which are necessary to investigate the effect of contrails and the influence SAFs have on these CoCiP is used. To be able to understand what the outputs of the program mean and what possibilities there are with the program, some basic knowledge about contrail cirrus, CoCiP and SAFs is explained.

2.1 Contrail cirrus

Contrails are the vapor trails produced by aircraft engines at high altitudes, where the exhaust gas of the aircrafts mixes with the surrounding air and builds ice crystals. The cover of the contrails cirrus is defined as the total cover of the total cirrus minus the cover of the cover natural cirrus [8]. Note that contrail cirrus is defined as contrails which persist over a certain time and spread over a larger area. They are cloud shaped, but differ in properties to natural cirrus clouds.

2.1.1 Effective radiative forcing

The contrail cirrus, respectively contrails play a significant role in Earth's radiative balance, which can be defined as the difference between absorbing and emitting outgoing longwave (LW) infrared radiation due to clouds or contrails. Earth also absorbs some radiation as well as cloud. These clouds also let some radiation through, but to investigate the influence of contrails those effects are not taken into account. This balance is quantified using a metric called radiative forcing (RF), which assesses the impact of various factors such as greenhouse gases, aerosols and contrails on Earth's energy balance by changing the amount of incoming solar radiation absorbed by the earth and the amount of infrared radiation emitted back into space [9]. The radiative forcing of contrails can be significant and can reach flux changes up to 100 W/m^2 locally and regional RF values close or above 1 W/m^2 [9].

To calculate the RF an example is given in figure 2.1. The contrails reflect 1 W/m^2 from the incoming solar radiation and reflect 3 W/m^2 from the outgoing radiation, which equals to an RF of 2 W/m^2. The positive result means, that the contrail is warming. Another measurement is the effective radiative forcing (ERF), which focuses more on the rapid adjustments like cloud cover because of contrails [11, 12]. Contrail cirrus, a type of persistent contrail that evolves into a more extensive cloud cover, plays a crucial role in RF associated with aviation activities. The difference in the two measurements can seen especially when looking at the effect of contrails, whereas investigating CO_2 it does not make a huge difference as you can see later on

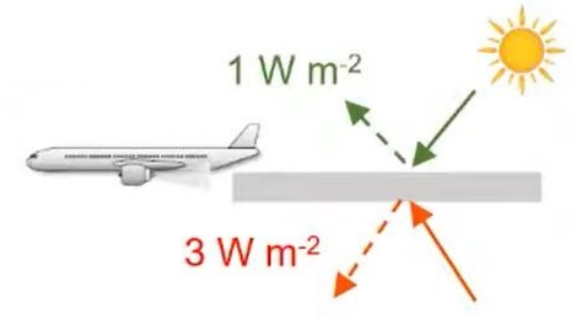

Figure 2.1: Example for the principle of RF [10]

[13]. Studies have shown that contrail cirrus contributes significantly to the overall radiative forcing linked to aviation making them an very important factor looking into the climate effect due to aviation [11, 12].

In 2018, it was also estimated, that contrail cirrus have even an larger impact to the annual mean RF than aviation's CO_2 and nitrogen oxides (NO_x) emissions, which makes it the biggest contributor to the RF of aviation [13].

Despite contrail cirrus exhibiting a higher nominal net RF compared to CO_2, its effect on global mean surface temperature change may be more complex [13]. Contrail cirrus tends to warm the upper troposphere, dehydrate the atmosphere and potentially reduce the occurrence and cloudiness of natural cirrus clouds. These secondary effects partially offset its warming impact [13].

The warming effect of contrail cirrus is depicted in Figure 2.2, alongside the emissions from aircrafts. These emissions include both CO_2 and non-CO_2 emissions such as NO_x, water vapor and sulfur. In the graph, the red and blue bars represent the best estimates of ERF for these emissions. Note that the red bars indicate a positive ERF, signifying a warming effect, while blue bars represent a cooling effect. Additionally, the whiskers denote the 5-95 % confidence intervals, indicating that the values fall within this range with a 90 % probability.

The figure illustrates that contrails exhibit a significantly higher ERF compared to CO_2 emissions. Moreover, the RF value is even larger than the ERF, owing to the secondary effects described earlier. Furthermore, the graphic highlights that other emissions, with the exception of the changes in ozone levels, have minimal impact compared to contrail cirrus. This underscores the importance of mitigating contrail formation from aircraft to address their significant climate impact [14] [10].

Despite the high RF and ERF values for contrails, they are both independent from the contrail's age. The lifetime of contrails however must be taken into account somehow, since their influence on the climate effect is crucial. Therefore, another measurement, respectively unit, is introduced, the energy forcing (EF). EF takes into account the cumulative energy which is trapped in the atmosphere due to the contrails formation and can be calculated by RF and the area of the contrails (length L(t) and width W(t)) by integrating it over the age of the contrail [10].

$$EF_{contrail} = \int_0^t RF \cdot L(t) \cdot W(t)\, dt \tag{2.1}$$

EF will be the main factor to look at during the analysis of the flights later on

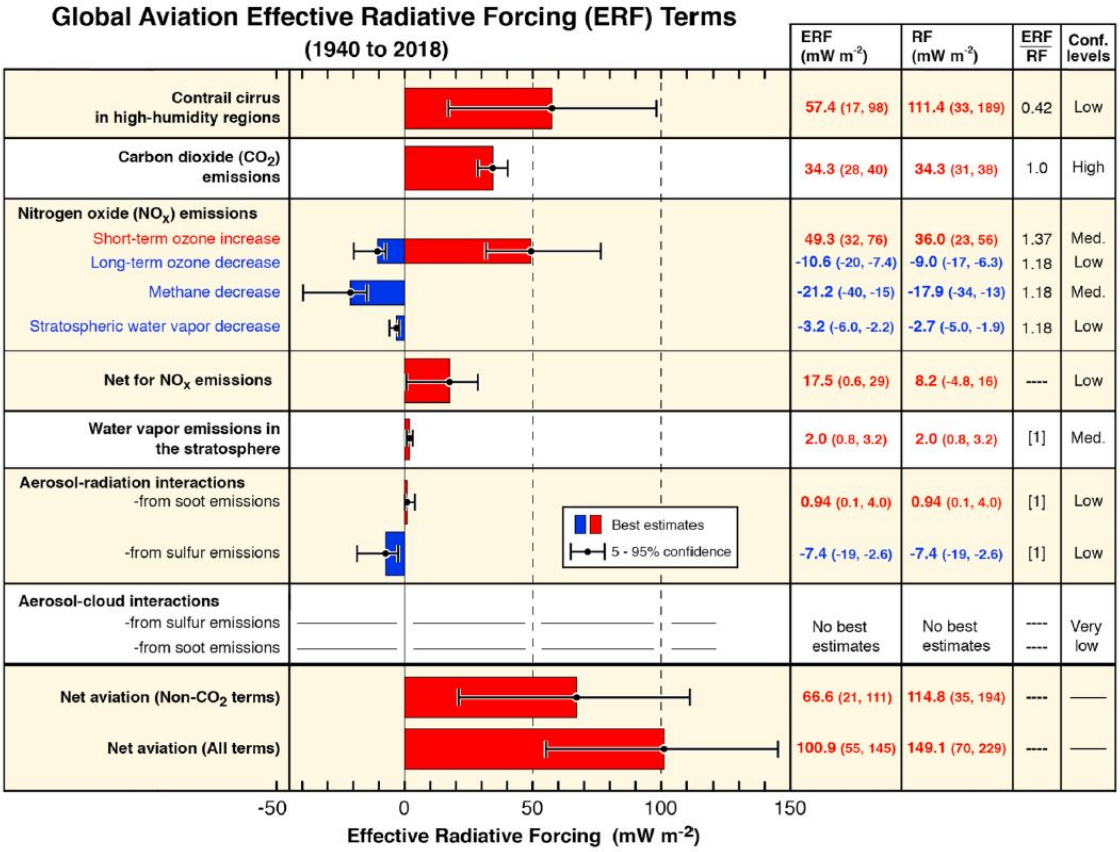

Figure 2.2: ERF and RF of different aviation pollutants [14]

since it takes the RF and the contrail age into account. The unit for EF is Joule. It is also possible to look at the EF per flight path, for which the EF needs to be divided by the length of the flights. However, to be able to understand the effect of the contrails it first of all is crucial to understand where and under which conditions the contrails form.

2.1.2 Contrail formation

The formation of contrails along flight paths depends on encountering ice-supersaturated conditions, which vary both spatially and temporally within the troposphere and tropopause region [5]. Ice-supersaturation refers to an atmospheric condition, where the relative humidity in the air with respect to ice exceeds 100 % [5]. Various factors such as humidity, shear, stratification, waves, turbulence and radiative heating then influence the characteristics of the contrails [5]. These conditions collectively create an environment, which can be conducive to the formation and persistence of contrails [5].

The basic principles behind contrail formation were independently established by E. Schmidt in 1941 and H. Appleman in 1953 [5]. Contrails form when the hot and moist exhaust gases from an aircraft engine mix with the cold and humid surrounding air. To really be able to form, certain circumstances must be fulfilled. One criterion that describes the necessary environment very well is the Schmidt-

Appleman criterion (SAC). It is an analytical method based on different factors to calculate the threshold temperature for contrail formation. These factors include engine efficiency, ambient temperature and humidity, exhaust temperature, and the water vapor emission index. This index describes the amount of emitted water per kg fuel and is crucial for the environmental effect of aviation. A more detailed definition can be found in further literature [13].

When this criterion is met, the mix of exhaust gas and surrounding air causes the humidity in the exhaust gas to surpass the saturation point for liquid water, resulting in many supercooled water droplets [5]. This water has to condense onto soot particles and atmospheric particles, which then continue to grow until they freeze [15]. These aerosol particles in the aircraft exhaust plume serve as nuclei for water condensation by deposition of water. This principle is also known as the "water-saturation constraint" [5]. By absorbing more water vapor from the surroundings, these water droplets grow rapidly, potentially resulting in the formation of visible contrails [5].

The frozen water droplets grow under favorable atmospheric conditions, especially when the atmosphere is supersaturated and temperatures are low [5]. These conditions are often present at typical cruise altitudes of 32,000 to 42,000 feet (9,800 to 12,800 meters) in effect ice supersaturated conditions [16]. The favourable conditions let ice particles form and grow, which can cause contrails existing out of hundreds of ice crystals per cubic centimeter of air [15]. The size of the crystals also can increase which mainly occurs when water condenses onto fewer particles, which then affects the contrails properties such as persistence and spread [15]. Additionally, there is a visibility constraint that estimates a minimum number of nucleated ice particles within contrails, typically around 10^4 per cubic centimeter within a plume age of 0.3 seconds [5].

The formation of ice particles in the exhaust jet, occurring within time scales ranging from 0.1 to 20 seconds, represents an initial stage in contrail formation [8]. Subsequent processes, such as wake vortices forming behind aircraft within time scales of 1 to 20 minutes and their transition into cirrus clouds, add further complexity to the modeling task [8]. Finally, the decay of contrails occurs within time scales ranging from less than an hour to possibly days, posing challenges for comprehensive modeling efforts [8].

2.1.3 Contrail properties

As already described before, contrails originate from the soot particles of the aircrafts in air masses that are saturated with ice. In theses conditions they expand and develop by absorbing surrounding water vapor [8]. This means, that the ice content within contrails can surpass the amount of water which was emitted from the aircraft, indicating that the surrounding conditions have a significant influence on the growth of the contrails [8].

Depending on the circumstances contrails can spread quickly across large areas, where high air traffic, increased humidity and thin cirrus clouds can be found. Those spreading contrails are refereed to as "contrail outbreak" [8]. Contrail outbreaks have a huge impact on the annual contrail coverage, which describes the surface

area which is covered by contrails. Therefore, it highlights the importance of local atmospheric conditions for contrail formation and aging [8].

Newly formed contrails are characterized by a high concentration of ice crystals. Those ice crystals typically can be seen within the plume with an age of 2 minutes [5]. Natural cirrus in comparison do not contain thousands of small ice particles per cubic centimeter like young contrails do [5]. The natural cirrus density of ice particles is a lot smaller, so the high density of ice crystals in contrail cirrus points out the unique nature of contrail formation and its potential impact on atmospheric properties [5].

The ice crystal number (N_i) is a crucial factor in contrail formation, influencing various properties such as persistence, spread and optical characteristics [5]. Higher N_i values lead to longer persistence, increased spread and brighter and more reflective contrails, which affect Earth's energy balance [5]. Furthermore, the processes of contrail and cirrus formation are nonlinear and heavily depend on ambient meteorological conditions and plume processes [8]. It is also possible, that short-lived contrails may even form in dry air under very low temperatures [8].

Observations of other studies have noted their presence also in ice-sub-saturated conditions, which indicates a more complex formation process [5]. In these conditions large ice particles were found, which exceeded 100 µm in diameter alongside smaller ice particles. This indicates a diverse particle distribution in the contrails [5]. The role of these large ice particles is unclear and would need further investigation, but this example shows the necessity for comprehensive research into contrail dynamics [5].

But besides that, they have the same attributes natural cirrus also posses. Parameters like the volume of contrail cirrus and total ice particle count are pivotal in quantifying the overall effect of contrails on atmospheric properties [5]. Different properties lead to different behaviors of contrails which then lead to different effects of the contrails.

2.1.4 Contrail effect

Longer lasting contrails have a higher impact to the global climate change especially when they form cirrus clouds [5]. They trap heat in the atmosphere due to a positive RF as described in chapter 2.1.1, just like high altitude clouds [5]. But they also have the possibility of cooling the atmosphere. The effect is depending on the properties of the contrails like the optical depth and ice crystal shape, but also time of the day and zenith angle of the sun[5].

In general all flights, commercial, military or other aircrafts, can increase the cloudiness due to the possibility of forming contrails and contrail cirrus clouds [5]. The LW RF is always positive and has the largest impact over a warm and cloud-free Earth surface, whereas short wave (SW) RF is mostly negative [5]. This effect can be seen the highest above unclouded dark surfaces, like the ocean [5]. Unlike CO_2 contrails are mostly only short-lived, because they only exist for hours or maybe a day, but never for weeks or years [15]. This indicates, that a reduction of contrails would have an immediate effect onto the Earth's climate [15].

Contrails are also not only building new cirrus, but can also increase already

existing cirrus and thicken them through generating more ice particles, when an aircraft crosses already existing clouds [5]. Both together, natural cirrus clouds and contrails cirrus, cover around 70% of the tropic and 30% of Earth's mid-latitudes if they are looked at a big scale [5]. In areas with high air traffic, for example Europe or the US east coast, the mean contrail cirrus cover can be up to 10% [13]. Earlier studie's found out that in Europe and at the east coast of the US only 12% of the flights cause 80% of the contrails, so a reduction of the contrail formation for those 12% would have a huge impact [13]. If, for example SAFs would be used in those 12% of flights the reduction could of RF could be measured immediately.

2.2 Sustainable aviation fuels

To be defined as a SAF, the fuel has to fulfill different criteria, which are stated by the International Civil Aviation Organization [4]. The first main criteria is, that the net life cycle greenhouse gas emissions need to be reduced by at least 10% compared to conventional fuels. Second is, that the SAF can not be produced from biomass in lands with high carbon stocks and third, that producing the SAFs is not influencing the local water, soil, air quality or food security. There are even more criteria that have to be fulfilled, but those three are the main points [4] [17]. SAFs can be produced out of a several number of sources like waste fats, municipal solid waste, wet waste and more [17].

There are several different pathways to produce SAFs (seven in 2022), but the most commonly used is the hydroprocessed ester and fatty SPK (HEFA-SPK), which also will be taken in this thesis as a reference. By now, the SAFs are blended with the conventional kerosene with up to 50% of SAF. If SAFs are used they can reduce the CO_2 emissions by up to 80% compared to conventional fuel [17]. But SAF is not only reducing the emissions of CO_2, but also the non-volatile particulate matter (nvPM) by up to 70%. The nvPM is the factor which mainly is responsible for building contrails, since it describes the soot emissions from an aircraft. Therefore, a use of SAF can significantly reduce the impact of the effect of contrails [4]. Since the particle number is reduced, the water freezes onto less particles, which for example leads to shorter lasting contrails, which then reduces the EF of the contrails. To simulate these effect a program called CoCiP is used.

2.3 Contrail Cirrus Prediction Model

CoCiP is a *python* program which is designed to forecast the formation and behavior of contrail cirrus clouds due to aircraft engine emissions. It was developed by Schumann in 2012 and is based on a Lagrangian approach [5]. It integrates numerical weather data to calculate the global distribution of contrails and contrail cirrus [5]. To be able to estimate the cirrus coverage and the climate impact of these, CoCiP simulates the entire contrail life cycle [8]. Contrails form in cold and humid air air along the flight paths of individual flights [8]. The properties of the contrails depend on the specific aircraft and their emission at different waypoints [8].

The model employs a Lagrangian Gaussian plume model to simulate the life cycle

of individual contrails, considering factors such as atmospheric conditions, aircraft properties and meteorological data [8]. In the model the contrail initiation is based on the SAC and on ambient humidity levels. With additionally information of wind, temperature, humidity and ice water data from numerical weather data the plume evolution can be simulated [8]. After CoCiP can estimate the RF of the contrails by analysing the contrail properties [8]. The results have been validated through comparisons with observations [18].

CoCiP incorporates various factors such as contrail formation thresholds, advection effects, turbulent mixing and ice mass formation from emitted and ambient humidity [5]. The number of ice crystals is influenced by the number of emitted soot particles [5]. The model uses simplified approximations for the survival of ice particles in adiabatically sinking wake vortices and the loss of particles in aged contrails. Contrails disappear when the bulk ice content sublimates or precipitates [8].

By utilizing numerical weather data to determine ambient meteorological conditions, CoCiP accurately simulates contrails in both global and specific scenarios [5]. CoCiP has been effectively applied to estimate the global climate impact of contrail cirrus and to explore mitigation strategies such as route optimization [8].

In summary, CoCiP serves as a valuable tool for forecasting contrail cirrus cloud formation and assessing their environmental impact. By combining advanced modeling techniques with observational data, CoCiP significantly contributes to climate research, which makes it the best fitting tool to analyze the impact of the use SAFs in aviation.

3
Methods

After taking a look at the basic methods and theory behind CoCiP, models with the provided data can be created. The first step therefore was to analyze, prepare and separate the data. Afterwards the the contrail models with the flight paths can be built.

3.1 Provided data and data preparation

The dataset for analysis was obtained upon request from the corresponding author [7]. It comprises essential flight data necessary for setting up a model in CoCiP. Each flight is uniquely identified by a flight ID, which allows an easy differentiation. Flight data is organized based on waypoints at various time intervals, with each containing longitude, latitude and aircraft altitude. Temperature readings corresponding to altitude are also included. All the values are measured at intervals ranging from 30 seconds to one minute.

Additionally, the dataset provides wind speed data in both horizontal and vertical directions, enabling the calculation of true wind speed. Geopotential and solar direct radiation values are available for each waypoint. Specific humidity readings are provided, along with true airspeed, aircraft mass, engine efficiency, fuel flow and burn rates, and thrust settings.

An essential aspect of the dataset is the measurement of the emission index (ei) for various pollutants such as NO_x, carbon monoxide (CO) and nvPM. Notably, nvPM is presented in two forms: nvPM_{ei_m}, representing mass emissions and nvPM_{ei_n}, indicating the number of emitted particles, both per kg fuel.

Furthermore, the dataset includes values for the NO_x induced temperature change per emitted NO_2 emission, accounted for NO_x efficacy effects (accf_{NO_x}) for Ozone (O_3), methane (CH_4) and primary mode ozone (pmo). These data enable CoCiP to calculate contrails for each flight, facilitating detailed analysis and modeling [7].

Another dataset was provided, containing comprehensive information on all flights for each day, including aircraft type, the timing of the first waypoint, departure and arrival airports with their respective countries, and more. To focus the analysis, only flights originating from Europe were considered.

Given the strong influence of atmospheric conditions on contrail formation, data from various dates needed to be examined. However, the dataset was limited to a single day, necessitating adjustments to reflect different dates. The original data was given for flights on the 1^{st} of July 2019. Additional dates were selected randomly, but also to ensure representation from each season. The chosen dates are as follows:

- 1^{st} of February 2019
- 8^{th} of March 2019
- 29^{th} of April 2019
- 13^{th} of August 2019
- 15^{th} of November 2019

3.2 Start with CoCiP

Following the separation and adjustment of the data, the CoCiP model was established and tailored accordingly. Initially, tutorials provided by *pycontrails.org* [19] were utilized to initiate the process. These tutorials were implemented using a subset of the available data, to get a grasp of the methodologies involved in CoCiP and the analytical capabilities it offers. Subsequently, the required codes for generating plots for the analysis were developed. The specifics of these codes will be elucidated in the subsequent section.

3.3 Models for different days

3.3.1 Selection of a time period

The initial aim was to identify time slots within the 24-hours of the 1^{st} of July where the EF attributable to contrails is at its peak. To achieve this, the dataset was segmented into two-hour blocks, with the starting time being a determining factor for each flight's inclusion in a particular block. These blocks commenced at intervals of two hours, such as from 0:00 to 2:00, 2:00 to 4:00, and so forth. Subsequently, blocks exhibiting the highest EF were singled out, along with additional time before and after these slots, ensuring comprehensive coverage of potential high EF periods. The selection of these time blocks can vary from day to day based on the specific values recorded.

Further subdivision of these two-hour blocks into 12-minute segments was made. This granular approach facilitated the construction of larger time periods by combining these segments.

Given the European Union's political objective, as discussed in Chapter 1.2, to achieve a 5 % share of SAF by 2030, the first analyzed time period was 1 hour and 12-minutes. Assuming a uniform distribution of flights throughout the day, this duration represents 5 % of the daily timeframe. Consequently, if 100 % SAF is used during this period while conventional fuel is used for the remainder of the day, the overall SAF share for the day would be 5 %. By employing this method daily over the course of a year, 5 % of the yearly fuel consumption would consist of SAF. For instance, to attain a 5 % SAF share using a blend of 50 % SAF and 50 % jet fuel, a time span of 2 hours and 24 minutes would be required. To compare the effects of different SAF blends and establish guidelines for their usage, various SAF-blends were examined. The selected SAF blends and their corresponding time periods required to achieve the same SAF quantity are presented in Table 3.1.

Table 3.1: Share of SAF and their associated time

share of SAF	Time
100 %	1 hour 12 minutes
75 %	1 hour 36 minutes
50 %	2 hours 24 minutes
25 %	4 hours 48 minutes
5 %	24 hours
0 %	24 hours

The baseline scenario of 0 % SAF usage serves as a reference point to assess the reduction in EF resulting from varying percentages of SAF utilization under identical atmospheric conditions. This reduction attributed to SAF deployment is evaluated over the entire day, enabling comparison across different fuel blends.

3.3.2 Calculation of the nvPM for different SAF-distributions

To establish an accurate model incorporating SAF distribution within CoCiP, the fuel needed to be set in CoCiP. The settings for the fuel were already given in CoCiP. Moreover, the nvPM, a key measurement provided in the dataset for jet fuel, must be recalculated for different SAF blends as it varies with their usage. To achieve this, the methodology outlined by Teoh [4] is employed. The formula for computing the new nvPM consists of two parts contingent on ΔH (the difference in hydrogen content in percentage points) between H_{blend} and H_{ref}. In this study, H_{ref} is set at 13.8 % [4], representing the hydrogen content of conventional jet fuel. For simplicity, the reference fuel is designated as jet fuel type A, referred to simply as jet fuel henceforth [4].

$$\Delta H = H_{blend} - H_{SAF} \tag{3.1}$$

The value of H_{blend} depends on the chosen blend, where p_{blend} specifies the mixture of jet fuel and SAF. Thus, H_{blend} can be calculated using the following formula, with H_{SAF} set at 15.3 % [4].

$$H_{blend} = H_{SAF} \cdot p_{blend} + H_{ref} \cdot 1/p_{blend} \tag{3.2}$$

Again the value for H_{SAF} can differ for different types of SAF. Here, as already described in chapter 2.2, HEPA-SPK is used as a reference [4]. This leads to the following equations for calculating the new nvPM-values:

When $\Delta H \leq 0.5$ %

$$nvPM_{SAF} = nvPM_{ref} \cdot (\alpha_0 + \alpha_1 \hat{F}) \cdot \Delta H \tag{3.3}$$

When $\Delta H > 0.5$ %

$$nvPM_{SAF} = nvPM_{ref} \cdot (\alpha_0 + \alpha_1 \hat{F}) \cdot \Delta H \cdot e^{(0.5-\Delta H)\cdot 0.5} \tag{3.4}$$

It's important to note that equation 3.4 was adjusted by adding "* 0.5" because the formula in the reference did not align with the plots provided. Based on this

observation, it was assumed that the plots were accurate, prompting the need to adapt the formula accordingly (see [4] and its supplementary information). Here, nvPM_{ref} represents the measured nvPM values from the provided dataset, while nvPM_{SAF} denotes the newly calculated values for the selected SAF blend. The coefficients α_0 and α_1 are originally defined by Brem et al. [20], with values of α_0 = -114.21 and α_1 = 1.06. $\hat{F}$ is defined as the thrust setting at each waypoint, also available in the provided dataset. With the updated nvPM values and the adjustments made in CoCiP, various plots can be generated and the EF can be calculated. To assess the reduction attributed to SAF, the total EF over the entire day is computed, facilitating comparisons among different fuel distributions. This means during the time with SAF use it is computed with the SAF distribution and the rest of the day with the reference jet fuel. This methodology is consistently applied across all selected days and various SAF and jet fuel mixtures.

3.4 Models for different flight paths

Another feasible approach for utilizing a specific quantity of SAF is to allocate it exclusively to certain flight routes. Initially, focus is placed on flight paths originating in Europe and terminating in North America (refer to the countries listed in the appendix A.2). To ensure equitable distribution of SAF akin to the various time blocks, the distance covered by flights from Europe to North America is set equal to the total kilometers flown by flights originating in Europe. This can be used to calculate the SAF blend to be used (see equations 3.5 to 3.6).

$$x_{100\ \%SAF} = x_{total} \cdot 5\ \% \tag{3.5}$$

$$p_{blendNA} = x_{100\ \%SAF} / x_{EU-NA} \tag{3.6}$$

Here x_{total} represents the total distance covered by flights originating in Europe, $x_{100\ \%SAF}$ denotes the distance that can be traveled using 100 % SAF, $p_{blendNA}$ indicates the blend to be used for flights between Europe and North America and x_{EU-NA} signifies the distance flown between Europe and North America.

Subsequently, a model is constructed to aggregate the total EF over the entire day. Initially, this is done with only jet fuel as a reference and then with the calculated blend. Afterwards, the reduction can be computed. To facilitate a more comprehensive comparison with the reduction method involving different SAF-blends, all previously analyzed days are also considered in the analysis of flight paths from Europe to North America.

Furthermore, an alternative approach involves focusing solely on flights originating and landing in Europe. This is motivated by the EU's establishment of regulations incentivizing the use of SAF in intra-European flights, offering monetary rewards to airlines for reducing their fossil CO_2 emissions by utilizing SAF [21]. Consequently, there is a strong likelihood that airlines will opt to utilize available SAF in intra-European flights. To analyze these flights, the same methodologies employed for flights from Europe to North America were applied.

3.5 Limitations

As already mentioned before, only flights with starting point in Europe were taken into account because of the regulations of the European Union. Some of the countries which are taken into account are not in the European Union, but they are also taken into account since they might orientate on these regulations too, e.g. Norway and Island. A full list of the countries can be found in the appendix (see A.1). It also needs to be mentioned, that the flight paths are exactly the same for all the different dates. This means, that it is not taken into account, that flight paths normally change in reality depending on the season or actual weather conditions, which can influence the EF. For examples if there is a storm with a lot of clouds during a changed date, it reduces the EF since the surface is covered already, whereas in reality the flight path might change to avoid the storm and results in a flight path over a free surface, which would result in a higher EF.

Additionally for some flights the point of origin, which means country and airport, are not given as well as for the destination. These flights were simply left outside of the analysis.

It also needs to be mentioned, that the fuels, jet fuel and SAF, are generalized. This means, there was no difference made in between different jet fuels or different types of SAF. Different fuels have different compositions, which can lead to slight difference between stored energy in the fuel or different exhausts of the plane engine, but they do not have a very huge impact. Therefore, jet fuel is set as low-sulfur-content Jet A and SAF is HEFA-SPK like described in Teoh [4].

4

Results

4.1 Time blocks for 1^{st} of July 2019

As outlined in Chapter 3, the initial step was to identify a time, where aircraft activity results in the highest contrail EF with jet fuel. To narrow the possible time down, first of all two hour blocks were created. Prior to generating contrails for each flight, the flight paths for the entire day originating from Europe were plotted, as depicted in Figure 4.1. This illustration highlights the busiest airspace, primarily concentrated above Europe. However, it also reveals numerous flights traversing the North Atlantic and heading towards Asia, with a smaller number bound for South America, Africa, and Oceania. Given that temperature, and consequently flight altitude, significantly influences contrail formation, as discussed in Chapter 2.1.2, it is expected that these longer flights are more prone to produce contrails compared to those originating and terminating within or near Europe, as their altitudes are generally lower.

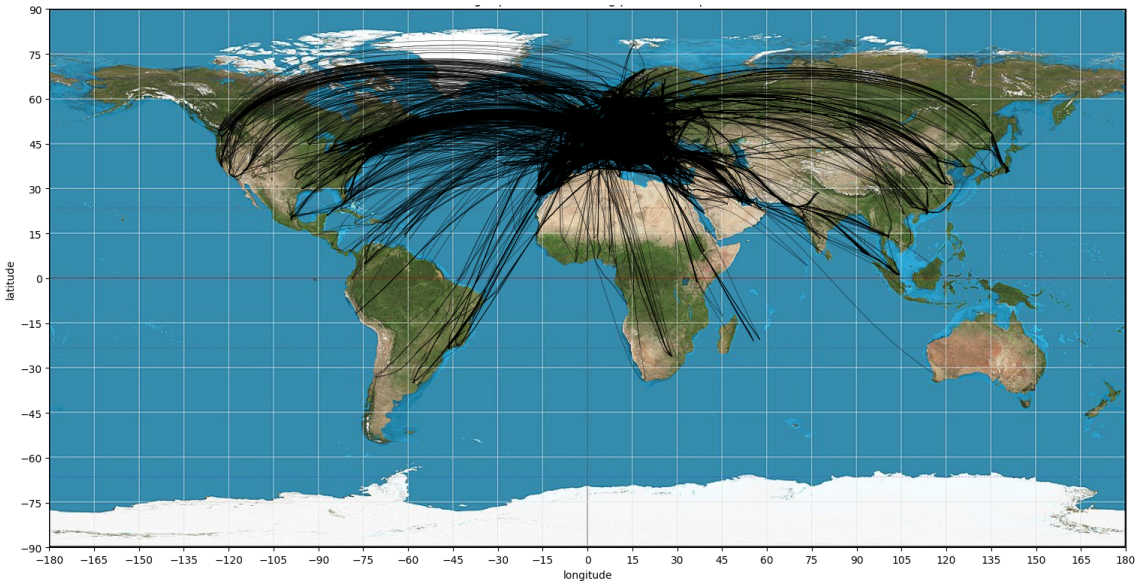

Figure 4.1: Flight paths of all flights originating Europe on July 1^{st}, 2019

The flights were initially categorized into two-hour blocks according to their start times (e.g., 0:00 to 2:00, 2:00 to 4:00, etc.). For each two-hour block, EF values were aggregated to determine the top four blocks with the highest values. An overview of these time blocks along with their corresponding EF is provided in Table 4.1.

Table 4.1: 2-hour time intervals and the total contrail EF within each interval

Time	**EF** $[1e^{12}$ J]
00:00 - 02:00	1071.95
02:00 - 04:00	-69.98
04:00 - 06:00	504.67
06:00 - 08:00	3397.71
08:00 - 10:00	6651.69
10:00 - 12:00	1965.78
12:00 - 14:00	4614.01
14:00 - 16:00	18838.50
16:00 - 18:00	19068.58
18:00 - 20:00	16237.79
20:00 - 22:00	22906.14
22:00 - 24:00	9304.98
Total	104491.82

As depicted in the table, the hours between 14:00 and 22:00 exhibit the highest EF. Particularly, the peak EF is observed from 20:00 to 22:00, reaching 22 906.14 $1e^{12}$ J. Following closely is the time block spanning from 16:00 to 18:00, with the second highest EF at 19 068.58 $1e^{12}$ J. The third block, from 14:00 to 16:00, records an EF of 18 838.50 $1e^{12}$ J, while the fourth block, covering 18:00 to 20:00, shows an EF of 16 237.79 $1e^{12}$ J. These four blocks stand out significantly from the others, with the closest EF in the 22:00 to 24:00 block with approximately 7000 $1e^{12}$ J less than the lowest of the four high blocks.

Additionally, it is notable that between 2:00 and 4:00, the EF becomes negative, recording at -69.98 $1e^{12}$ J, indicating that contrails cool the atmosphere during this period on average. To delve further into the positive EF, the data within the 8 hours with the highest EF are examined more closely. Time blocks of 12 minutes each were created for these 8 hours, along with an additional 24 minutes before and 1 hour and 24 minutes after, to ensure no possible high EF occurrences are overlooked. The complete results are presented in the Appendix (A.3), with a portion of the data showcased in Table 4.2, highlighting segments with the highest EF values.

By dividing the data into 12-minute time blocks, they can easily be used to create a block with larger time intervals. For instance, six consecutive 12-minute blocks can be combined to form a block lasting 1 hour and 12 minutes. For the 1 hour and 12 minute blocks, which are required for the 100 % SAF blend, intervals with a 12-minute difference can be overlaid, resulting in blocks, which are overlaying by 1 hour. A portion of this data is presented in Table 4.3, which highlights the time period with the highest EF value occurring between 20:48 and 22:00, registering at 17 206.45 $1e^{12}$ J. During this interval, a 100 % SAF blend can be utilized, achieving a 5 % SAF share throughout the day.

For a blend comprising 75 % SAF and 25 % conventional jet fuel, a time block of 1 hour and 36 minutes is required to maintain the 5 % SAF share over the entire day, or the same amount of SAF as in a 100 % SAF blend over 1 hour and 12 minutes.

Table 4.2: 12 minute time blocks and EF of the total contrails in the block

Time	EF [$1e^{12}$ J]
20:00 - 20:12	1100.21
20:12 - 20:24	1874.97
20:24 - 20:36	2151.84
20:36 - 20:48	572.69
20:48 - 21:00	3453.46
21:00 - 21:12	3525.26
21:12 - 21:24	3656.78
21:24 - 21:36	2120.09
21:36 - 21:48	3166.05
21:48 - 10:00	1284.81
10:00 - 10:12	2271.69
10:12 - 10:24	2952.13
10:24 - 10:36	452.08
10:36 - 10:48	923.42
10:48 - 11:00	271.79

Table 4.3: 1 hour 12 minutes time blocks with an 1 hour overlay and EF of the total contrails in the block

Time	EF [$1e^{12}$ J]
20:00 - 21:12	12678.43
20:12 - 21:24	15235.00
20:24 - 21:36	15480.12
20:36 - 21:48	16494.33
20:48 - 22:00	17206.45
21:00 - 22:12	16024.68
21:12 - 22:24	15451.55
21:24 - 22:36	12246.85
21:36 - 22:48	11050.18
21:48 - 23:00	8155.92

Similarly, a 50 % SAF blend necessitates a time block of 2 hours and 24 minutes, while a 25 % blend extends to 4 hours and 48 minutes. Another strategy involves evenly distributing the 5 % SAF over the entire day. For reference, models are also constructed using 100 % jet fuel within the selected time slots.

The chosen time intervals corresponding to the highest EF for the different blends are summarized in Table 4.4. Detailed tables outlining the selection of these time spans are provided in the appendix (Table A.4 - Table A.7).

Table 4.4: SAF-blends and their time blocks for highest EF and EF with jet fuel

SAF-blend	Time	EF [$1e^{12}$ J]
SAF 100	20:48 - 22:00	17206.45
SAF 75	20:48 - 22:24	22430.27
SAF 50	19:24 - 21:48	28423.12
SAF 25	17:36 - 20:24	47993.21
SAF 5	00:00 - 24:00	104491.82

4.2 Contrails for the 1^{st} of July 2019

4.2.1 100 % SAF

The primary fuel utilized for flights is the jet fuel, a standard fuel type also incorporated in CoCiP. The initial phase of the analysis entailed creating a plot with jet fuel as the baseline and computing the total EF during the timeframe from 20:48 to 22:00, yielding a value of 17 206.45 $1e^{12}$ J. The geographical distribution of contrail formation locations is depicted in figure 4.2.

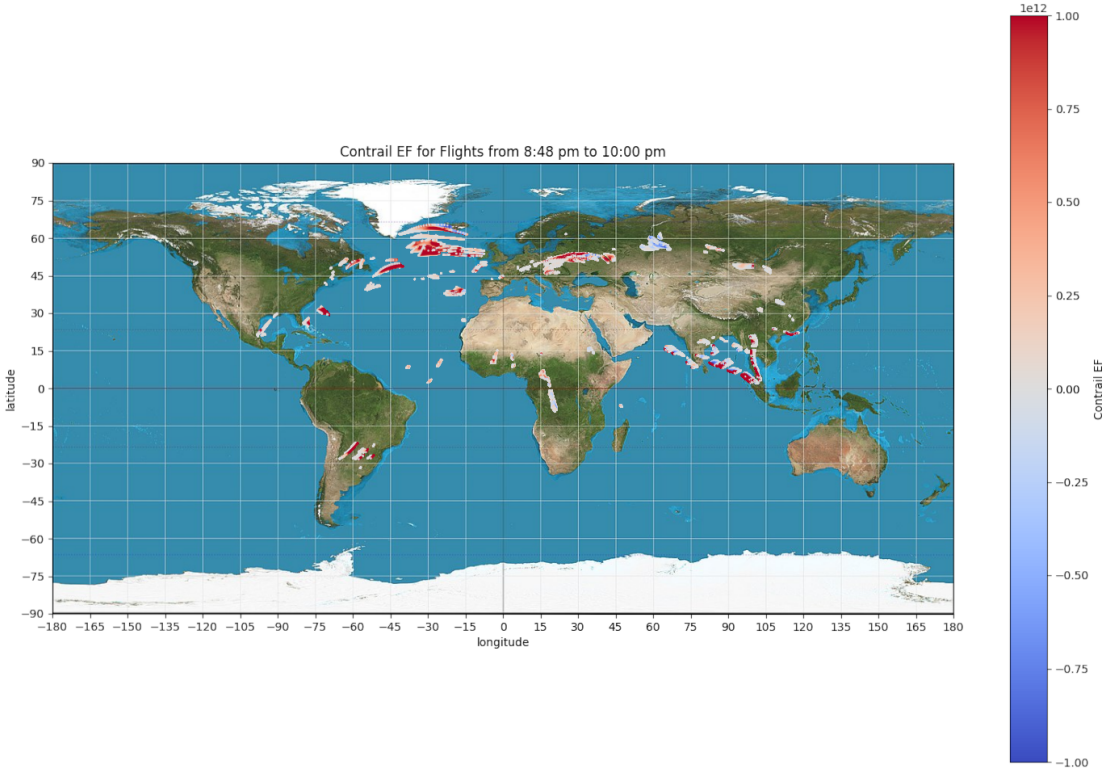

Figure 4.2: EF of contrails due to flights with starting time between 8:48 pm and 10:00 pm, 1^{st} of July 2019, with starting point in Europe; Fuel: Jet fuel

Figure 4.2 provides insights into the distribution of contrails, showcasing a predominance of positive EF. These instances, represented by red dots, are notably concentrated over eastern Europe (15° to 30° longitude and 45° to 60° latitude) and the North Atlantic (-45° to -15°; 45° to 75°). Similarly, positive EF is observed along the east coast of North America (-75°; 30°), in the middle south of South America (-60°; -30° to -15°) and between India and Indonesia (75° to 105°; 0° to 15°). Additionally, smaller contrails with minimal effects are discernible. While some small positive EF can be spotted in Russia, the figure also depicts negative EF in this region due to contrails. Nevertheless, apart from this area, negative EF contrails are absent. Many of the formed contrails, represented as grey dots in figure 4.2, have only small to zero impacts on the total EF.

The formation of contrails is linked to the nvPM_{EI_n}. During the specified time

frame with jet fuel, the mean nvPM$_{EI_n}$ for each waypoint averages 1037.65 $1e^{12}$ particles per kg fuel. This value indicates the emission of this quantity of particles per kg fuel on average at each waypoint. The average contrail lifetime with jet fuel is calculated to be 6.02 hours, with contrails originating from 16.97 % of the flights. Considering the variation in flight paths and distances between waypoints, the EF per flight distance is calculated to be 4 524.38 $1e^3$ J m^{-1}.

Transitioning to the simulation of the same flights using 100 % SAF, it is notable that the regions where contrails are formed remain consistent (see figure 4.3). Similarly, the color indications, signifying the strength of contrails, remain largely unchanged. However, with 100 % SAF as fuel, the total EF reduces to 12 589.39 $1e^{12}$ J, resulting in an EF per flight distance of 3 054.8 $1e^3$ J m^{-1}. This means a reduction is present, but it can not be seen in the plot. Additionally, the mean nvPM$_{EI_n}$ decreases to 460.85 $1e^{12}$. With 100 % SAF, the mean contrail age between 20:48 and 22:00 is determined to be 5.56 hours, with contrails forming due to 19.97 % of the flights.

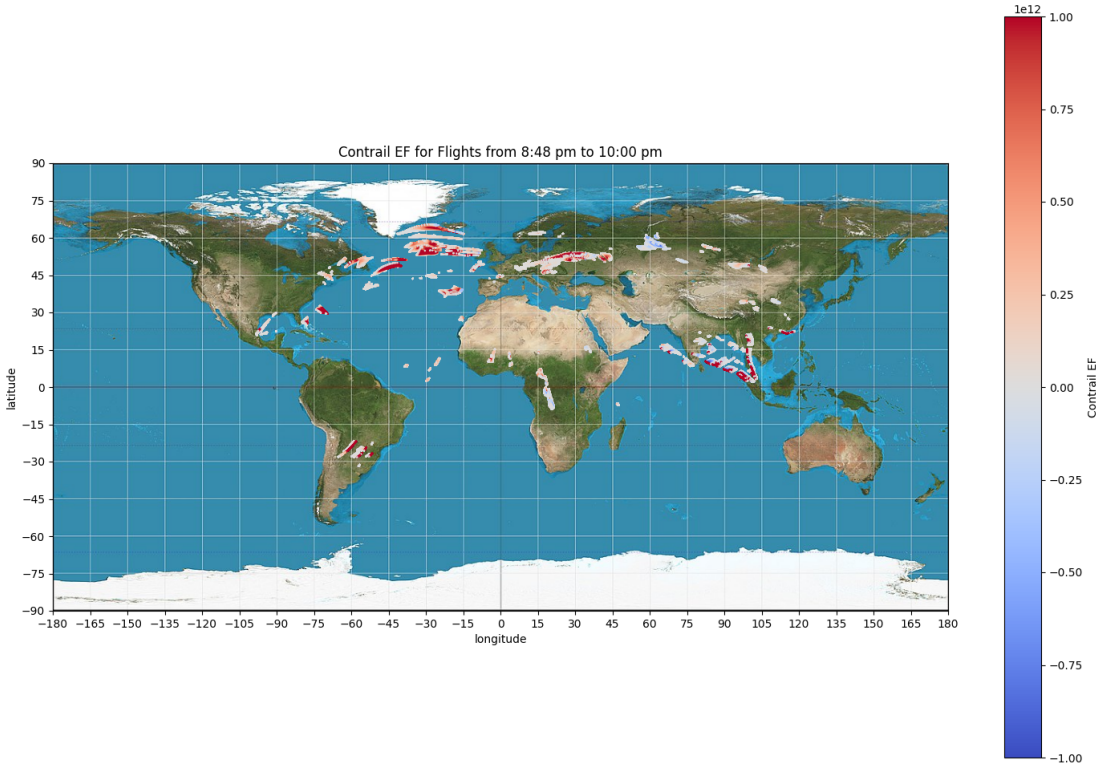

Figure 4.3: EF of contrails due to flights with starting time between 8:48 pm and 10:00 pm on the 1st of July 2019 with starting point in Europe; Fuel: 100 % SAF

In the end this leads to a reduction of 4 617.06 $1e^{12}$ J. This means a use of 100 % SAF in 1 hour and 12 minutes where the highest EF occurs, reduces the total EF over the day to 99 874.78 $1e^{12}$ J. For the reference of only using jet fuel, the total EF of the day is 104 491.82 $1e^{12}$ J. This concludes to a reduction of 4.42 % compared to the initial model with only jet fuel.

4.2.2 75 % SAF

If 75 % SAF and 25 % jet fuel is used, the time span expanse to 1 hour and 36 minutes to use the same amount of SAF. The expansion and adjustment of the analyzed time period also influences the contrail formation. However, since the time only extends by 24 minutes compared to the duration of using 100 % SAF and has the same starting time, the plot remains largely unchanged (A.1). The extend results in a total EF of 22 430.25 $1e^{12}$ J during the selected time period, equating to a contrail EF per flight distance of 5 045.55 $1e^{3}$ J m^{-1} considering all flights' lengths during that period with jet fuel type A. These contrails are generated by 17.44 % of the flights and have an average lifetime of 5.92 hours. The mean $nvPM_{EI_n}$ value for the period between 20:48 and 22:24 is 1 044.49 $1e^{12}$ particles per kg fuel.

Using a fuel blend comprising 75 % SAF and 25 % jet fuel, the mean $nvPM_{EI_n}$ decreases to 519.17 $1e^{12}$ particles per kg fuel. With an average lifetime of 5.67 hours, contrails are formed by 19.70 % of the flights. The EF per flight distance is calculated to be 3 568.9 $1e^{3}$ J m^{-1}, resulting in a total EF of 16 778.85 $1e^{12}$ J and therefore a reduction of 5 651.42 $1e^{12}$ J. Over the whole day the EF decreases from the original 104 491.82 $1e^{12}$ J to 98 840.40 $1e^{12}$ J, which is a reduction of 5.41 %.

4.2.3 50 % SAF

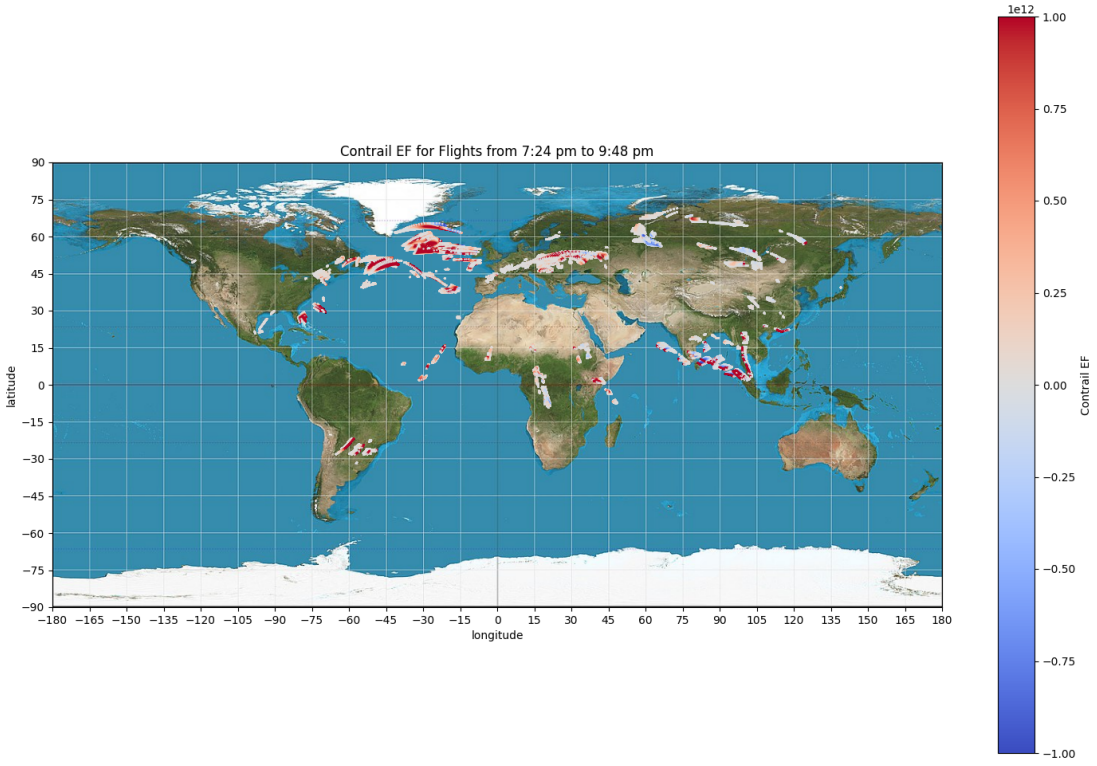

Figure 4.4: EF of contrails due to flights with starting time between 7:24 pm and 9:48 pm on the 1^{st} of July 2019 with starting point in Europe; Fuel: Jet fuel

The time allocated for using 50 % SAF and 50 % jet fuel spans from 19:24 to 21:48. When utilizing only jet fuel, the total EF reaches 28 423.10 $1e^{12}$ J, with an

average nvPM$_{EI_n}$ value of 1 138.81 $1e^{12}$ particles per kg fuel. This equates to a mean EF per flight distance of 2 881.28 $1e^{3}$ J m^{-1}. On average, contrails persist for 4.71 hours and are generated by 15.48 % of flights. Figure 4.4 illustrates the contrails in this time block. Areas with a high density of high EF, such as the North Atlantic (-75° to -15°; 45° to 75°) and the eastern part of Europe (15° to 30°; 45° to 60°), remain consistent with previous time slots for SAF use of 100 % and 75 %. However, the area over the North Atlantic has expanded, showing more red dots, which means this area causes a higher EF because of the expanded time frame. The airspace between India and Indonesia (60° to 105°; 0° to 15°), the southern part of South America (-60°; -30° to -15°), and the east coast of North America (-75°; 30°) remains comparable to previous time blocks. Additionally, positive EF can be observed in the east of Africa (45°; 0°) and along the west coast of Africa (-30° to -15°; 0° to 15°). In Russia and China (60° to 135°; 45° to 75°), the number of contrails has increased, but they are mostly only slightly positive or negative. Also, the number of contrails with a small impact has notably increased in this area.

Using 50 % SAF reduces the mean nvPM$_{EI_n}$ to 679.52 $1e^{12}$, resulting in a total EF of 21 559.31 $1e^{12}$ J or 2 138.7 $1e^{3}$ J m^{-1}. Contrails persist for an average of 4.64 hours and are formed by 16.84 % of flights. This results in a total EF of 97 628.03 $1e^{12}$ J over the whole day, which is a reduction of 6.57 % compared to the EF with jet fuel.

4.2.4 25 % SAF

By extending the time span even further, from 17:36 to 22:24, totaling 4 hours and 48 minutes, the overall EF also sees an increase. The total EF amounts to 47 993.19 $1e^{12}$ J, resulting in 2 823.30 $1e^{3}$ J m^{-1}. The average nvPM$_{EI_n}$ is 1 230.98 $1e^{12}$ particles per kg fuel. Contrails are formed by 15.63 % of flights, with an average duration of 4.43 hours. The areas where contrails occur remain consistent with those described previously, but with a higher density of points due to the extended time span, especially noticeable over Europe, the North Atlantic, Russia, and between India and Indonesia. Additionally, some areas with minimal EF can be observed, such as in the south of Africa, for example (see figure 4.5).

When 25 % SAF is utilized during that period, the average EF per flight distance amounts to 2 450.23 $1e^{3}$ J m^{-1}, totaling 41 589.37 $1e^{12}$ J. These contrails persist for an average of 4.37 hours and are formed by 16.24 % of flights. The mean nvPM$_{EI_n}$ value is 947.87 $1e^{12}$ particles. In the end it is a decrease by 6.13 % and results in 98 087.98 $1e^{12}$ J over 24 hours.

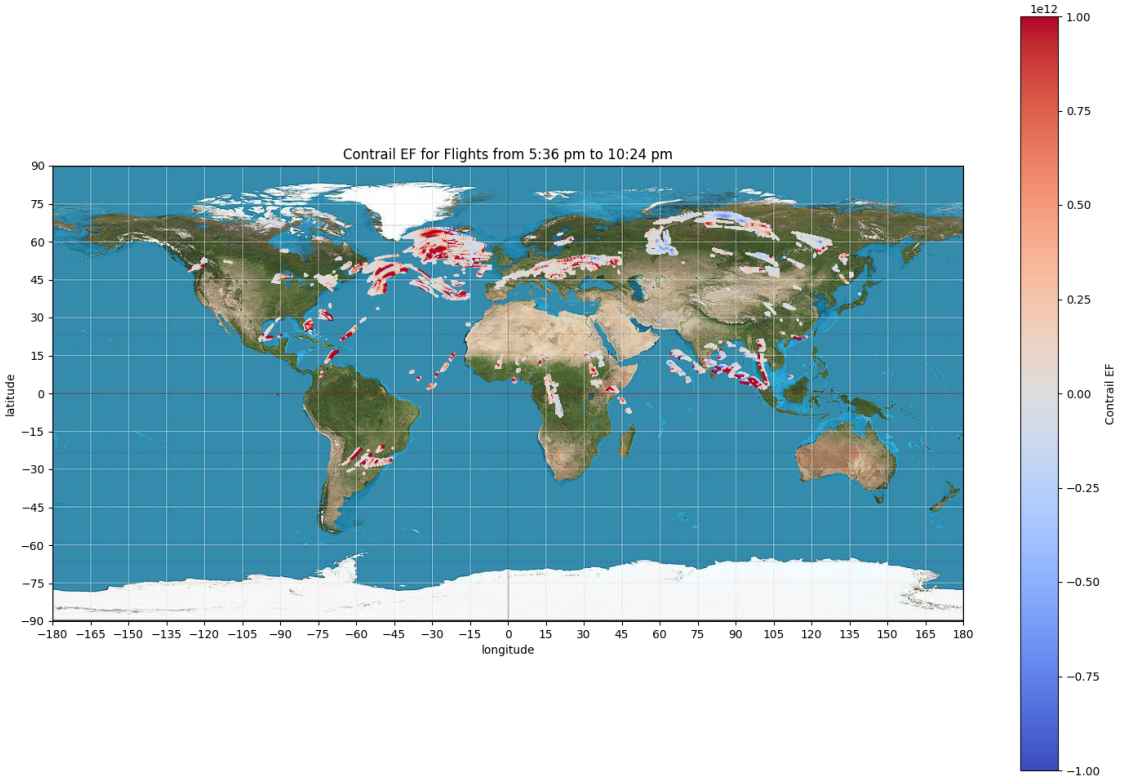

Figure 4.5: EF of contrails due to flights with starting time between 5:36 pm and 10:24 pm on the 1^{st} of July 2019 with starting point in Europe; Fuel: Jet fuel

4.2.5 5 % SAF

The last model utilized a blend of 5 % SAF and 95 % jet fuel throughout the entire day. However, due to insufficient computer RAM, the contrail plots had to be separated into two-hour blocks for analysis. Ultimately, this approach yielded a total EF of 101 212.03 $1e^{12}$ J over the entire day with the SAF blend, equivalent to 860.67 $1e^{3}$ J m^{-1}. Approximately 8.22 % of flights contributed to contrail formation, with an average duration of 5.23 hours. The nvPM$_{EI_n}$ count for this blend stood at 1 585.76 $1e^{12}$ particles per kg fuel, only marginally lower than the count with jet fuel alone, which was 1 628.02 $1e^{12}$ particles per kg fuels. In comparison, the reference model using 100 % jet fuel exhibited an EF of 104 491.82 $1e^{12}$ J, translating to an EF per flight distance of 888.56 $1e^{3}$ Jm^{-1}. With jet fuel alone, the contrails were formed by 8.14 % of the flights, lingering for an average of 5.26 hours in the atmosphere.

4.3 Results for the additional dates

To diversify the analysis and ensure the findings, additional dates (1^{st} of February, 8^{th} of March, 29^{th} of April, 13^{th} of August and 15^{th} of November 2019) were examined using the same methodology. With each date change, the meteorological conditions varied, consequently altering the timeframes with the highest EF for different SAF-

blends. Additionally, the geographical areas impacted by contrails shifted due to varying weather conditions. While the specifics of these areas are not elaborated to prevent unnecessary lengthening of this thesis, it is noted that flight paths remained consistent across the days, influencing contrail occurrence areas. An overview of the data for these different days is provided in Table 4.5. Notably, the analysis for the 1^{st} of July is also included in the table for completeness.

The table is divided into five sections, each corresponding to a different SAF-blend. Within each section, the dates analyzed are listed alongside the respective time slot with the highest EF, such as 1 hour and 12 minutes for 100 % SAF. The third column displays the total EF for the day. For jet fuel, this value represents the original calculated EF over the entire day without SAF use. To compute the EF over the whole day with SAF utilization, the EF of the time slot was determined with SAF use, while the remainder of the day utilized conventional jet fuel. This methodology enables comparison across all results for different SAF-blends and different days, facilitating assessment of both absolute reduction in Joules and reduction in percentage relative to the EF of the day.

When considering the total EF throughout the entire days with jet fuel, it is evident that the 15^{th} of November stands out with a total EF exceeding 210 000 $1e^{12}$ J. Following this, the 1^{st} of July exhibits the second highest EF, at approximately 105 000 $1e^{12}$ J, not even half of the 15^{th} of November's EF. The 1^{st} of February ranks third with a total EF value of around 89 000 $1e^{12}$ J for the entire day. Subsequent dates, namely the 8^{th} of March, 29^{th} of April, and 13^{th} of August, show total EF values ranging from approximately 30 000 to 12 000 $1e^{12}$ J. These values are visually depicted in Figure 4.6 for clarity.

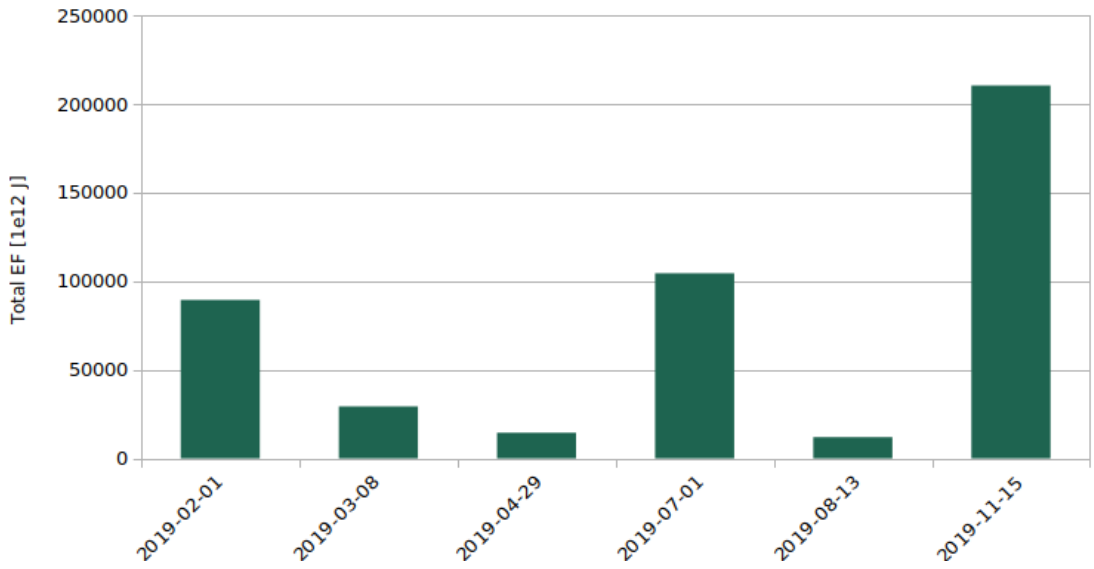

Figure 4.6: Overview of the total EF with jet fuel of the different analyzed days

A higher total EF for the entire day correlates with a greater EF during the time slot exhibiting the highest EF of the day, consequently resulting in a higher potential for EF reduction through SAF utilization. For instance, the absolute reduction on the 15^{th} of November surpasses 17,000 $1e^{12}$ J for a 100 % SAF blend, whereas the

total EF over the whole day on the 13^{th} of August is only 12,000 $1e^{12}$ J, marking a 5 000 $1e^{12}$ J difference compared to the absolute reduction on the 15^{th} of November. This observation suggests that the lowest absolute reduction is evident on the day with the lowest total EF value, namely the 13^{th} of August. On this particular day, the total reduction ranges from 232.60 $1e^{12}$ J with a 5 % SAF use throughout the entire day to 861.57 $1e^{12}$ J, where SAF is employed between 19:12 and 21:48 with a blend of 50 % SAF and 50 % jet fuel. For a graphical representation of the absolute reduction values, refer to Figure 4.7.

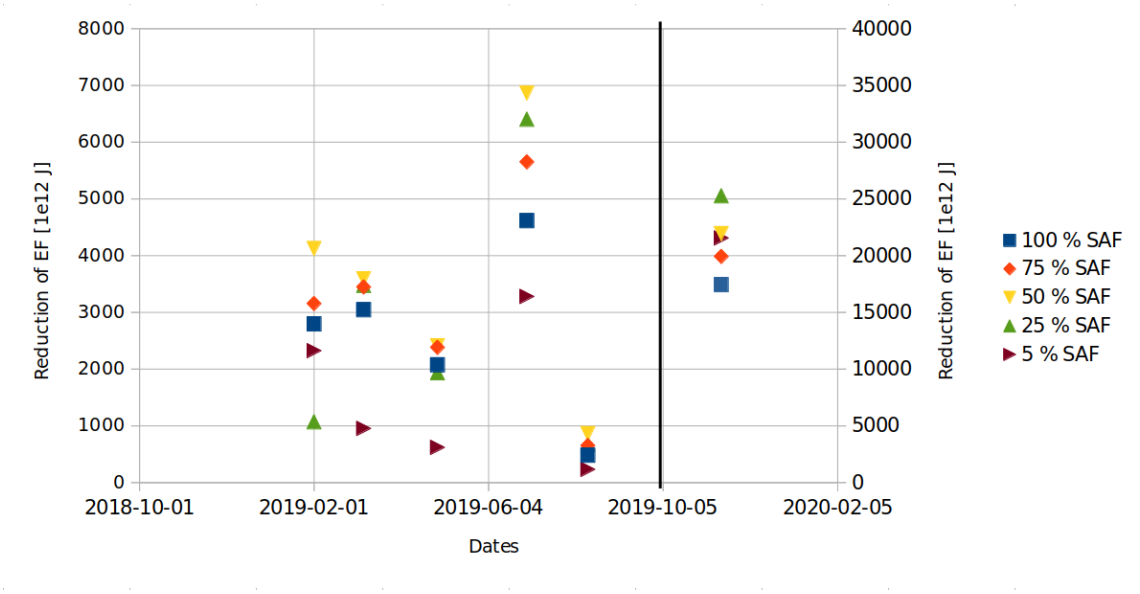

Figure 4.7: Absolute reduction due to use of different SAF-blends

Note that in the figure, the first five dates are aligned with the left y-axis, while the 15^{th} of November is associated with the right y-axis, distinguished by the black line. Both axes represent the absolute reduction of EF resulting from the use of different SAF-blends, measured in $1e^{12}$ J. The rationale behind separating the y-axes is to enhance the visibility of differences among the first five dates, as the reduction on the 15^{th} of November significantly exceeds that of the other days.

Figure 4.7 demonstrates that, in most cases, the blend comprising 50 % SAF and 50 % jet fuel yields the highest absolute reduction, ranging from 861.57 $1e^{12}$ J on the 13^{th} of August to 6 863.79 $1e^{12}$ J on the 1^{st} of July. On the 15^{th} of November, this blend achieves an approximate reduction of 22 000 $1e^{12}$ J, but the blend with 25 % SAF and 75 % jet fuel achieves an even higher reduction of over 25 000 $1e^{12}$ J. This 25/75 blend also demonstrates a notable reduction on the 1^{st} of July, nearly matching the reduction of the 50/50 blend and ranking as the blend with the second highest reduction. It also ranks second in reduction on the 8^{th} of March, 29^{th} of April, and the 13^{th} of August. However, on the 2^{nd} of February, it yields the lowest reduction among all the different possible SAF-blends, at only 1 071.22 $1e^{12}$ J.

Using a 100 % SAF blend consistently results in a reduction that generally falls in the middle range of the possible blends. However, on the 15^{th} of November, it represents the blend with the lowest possible reduction, at 17 444.28 $1e^{12}$ J.

On all other days except the 15^{th} of November and the 2^{nd} of February, the blend

with the lowest reduction is 5 % SAF and 95 % jet fuel. On the 2^{nd} of February, it ranks as the blend with the second lowest reduction, while on the 15^{th} of November, it lies in the middle. The blend with 75 % SAF and 25 % jet fuel fluctuates between the second highest and second lowest positions in reduction on different days.

It is also insightful to examine the reduction relative to the total EF of each day, as presented in Table 4.5. The order of the different SAF-blends remains consistent on each day. Reduction relative to the total EF ranges from only 1.20 % on the 2^{nd} of February with a blend of 25 % SAF and 75 % jet fuel to 16.68 % on the 29^{th} of April with a blend of 50 % SAF and 50 % jet fuel.

4.4 Flights from Europe to North America

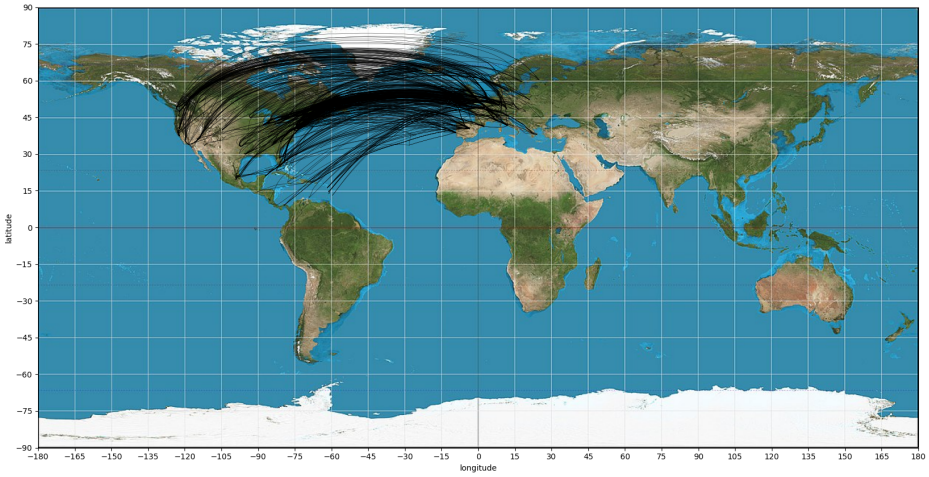

Figure 4.8: Flight paths from Europe to North America on the 1^{st} of July 2019

The analysis of July 1st revealed that a significant number of high EF contrails form over the North Atlantic, suggesting that flights from Europe to North America contribute substantially to the day's EF. Therefore, an alternative approach to utilizing the available SAF is to allocate it exclusively to flights between Europe and North America. The flight paths for these journeys are depicted in Figure 4.8.

To ensure consistent SAF usage as in the previous analysis, it is necessary to determine the appropriate proportion of jet fuel and SAF to load onto airplanes for flights from Europe to North America. This calculation is based on the total flown kilometers. The total distance covered by flights originating from Europe is 34 686 220.00 km. With a 5 % SAF share, this would allow for a distance of 1 734 311.00 km to be flown using 100 % SAF. Now, the total distance of the flights from Europe to North America is 5 877 306.88 km, accounting for 16.94 % of the total flown kilometers. Thus, the calculation results in a SAF-blend of 29.51 % SAF

and 70.49 % jet fuel to maintain the targeted 5 % SAF usage throughout the day for all flights.

Before constructing the model with the SAF-blend, a reference model using only jet fuel was created to facilitate comparison of the reduction achieved by SAF usage. To ensure robustness, the analysis leveraged data from the six days examined previously, allowing for the creation of an average and comparison with the previous study's findings. Figure 4.9 illustrates the contrails formed by flights between Europe and North America, using the flight paths from July 1^{st} and meteorological data from March 3^{rd} as an illustrative example.

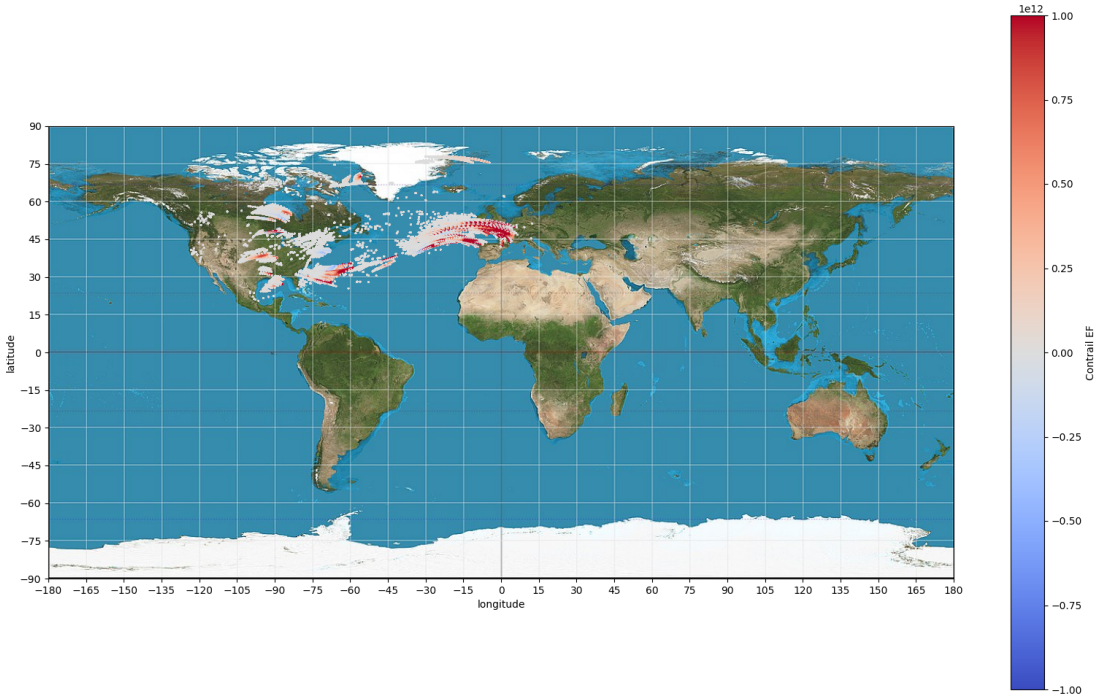

Figure 4.9: Contrails due to flights from Europe to North America on the 3^{rd} of March 2019 with jet fuel

It is evident that contrails predominantly occur along the flight paths between Europe and North America, with the highest impact seen over the North Atlantic close to Europe (-30° to 0° longitude and 30° to 60° latitude), as well as along the east coast of North America (-75° to 60°; 30°). While some contrails contribute to significant warming effects, others have a negligible impact or even cause cooling. This variation can be attributed to factors such as weather conditions, sunlight, and time of day, as contrails can persist for more than 24 hours. It is important to note that the distribution and impact of contrails can vary greatly between days.

Upon establishing the reference case for each day, it becomes apparent that flights from Europe to North America contribute significantly to the overall EF. Figure 4.10 illustrates the proportion of EF from flights between Europe and North America compared to the total EF of flights originating from Europe. Notably, on the 8^{th} of August, this share is approximately 10 %, indicating a relatively lower impact

compared to other days where the share ranges between 33 % and 67 %. This disparity highlights the substantial influence of transatlantic flights on overall contrail formation.

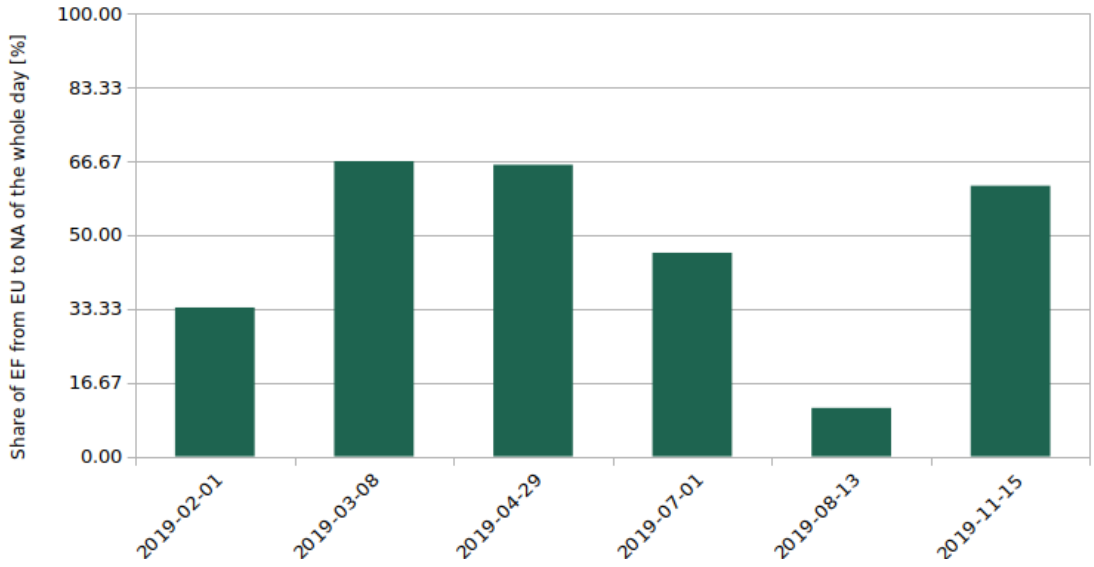

Figure 4.10: Share of EF of the flight from Europe to North America of the EF of the whole days

A significant portion of the total EF indicates a substantial potential for contrail reduction through SAF utilization. Employing a blend of 29.51 % SAF uniformly across all flights from Europe to North America results in a reduction of the EF of the contrails ranging from 10 % to 24 % (except in August, where it is 4.33 %). On average, including August, this reduction amounts to 14.65 % of the total EF, computed by averaging the percentage reductions of each day. Alternatively, averaging the total EF of each day (62 639.71 $1e^{12}$ J) with the absolute reduction of each day (14 044.67 $1e^{12}$ J) yields an average reduction of 18.31 %.

4.5 Inter european flights

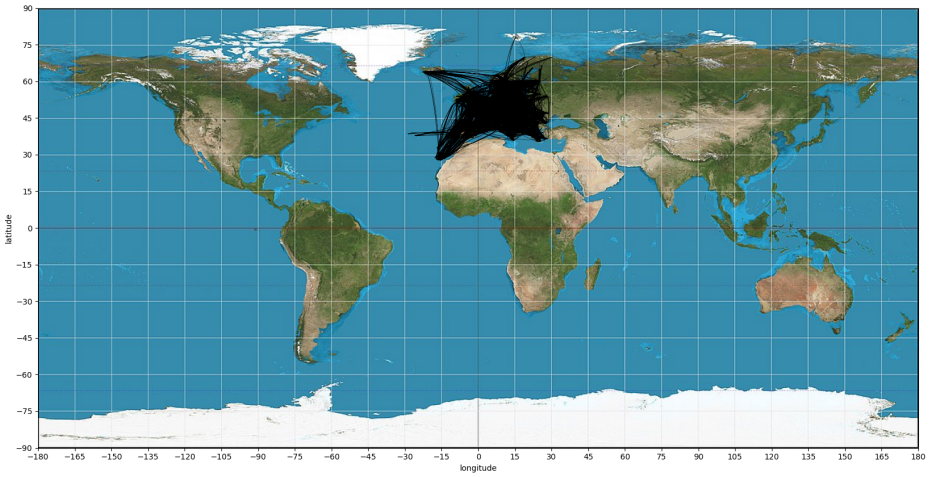

Figure 4.11: Flight paths starting and ending in Europe on the 1^{st} of July 2019

Despite differences in flight patterns compared to transatlantic flights, analyzing flights within Europe is still crucial due to the incentives airlines receive for reducing CO_2 emissions, as outlined in Chapter 3.4. Additionally, the volume of intra-European flights is substantial, with 15 097 flights recorded on the 1^{st} of July alone. The total distance covered by these flights amounts to 18 003 621.57 km, representing 51.90 % of the total distance flown by all flights originating from Europe. Flight paths for these intra-European flights are illustrated in Figure 4.11.

Using the same calculation method, which was used for the flights from Europe to North America, results in a blend of 9.63 % SAF and 90.37 % jet fuel. This blend is potentially used evenly for all the flights inter european. Using that blend only reduces the total EF over the day by 0.38 % in average, which equals 306.33 $1e^{12}$ J. Even the highest reduction on the 1^{st} of February with 1.32 % is still very low. The lowest reduction can be found on the 29^{th} of April with only 5.3 $1e^{12}$ J, which in the end is only 0.04 % of the total EF.

The examination of contrails reveals that intra-European flights have a minimal impact on the overall contrail EF. For instance, scrutinizing contrails from the 8^{th} of March indicates that strongly warming contrails are predominantly observed over France, the northern coast of Spain (-15° to 15°; 45° to 60°), and Ukraine (15° to 30°). Additionally, there are regions, such as the eastern coast of Norway and Eastern Europe, where contrails have negligible effects (refer to Figure 4.12).

This observation is further supported by the EF values. With jet fuel, intra-European flights contribute between 2.70 % (on the 8^{th} of March) and 25.60 % (on the 1^{st} of February) to the total EF for the day. However, considering the distance

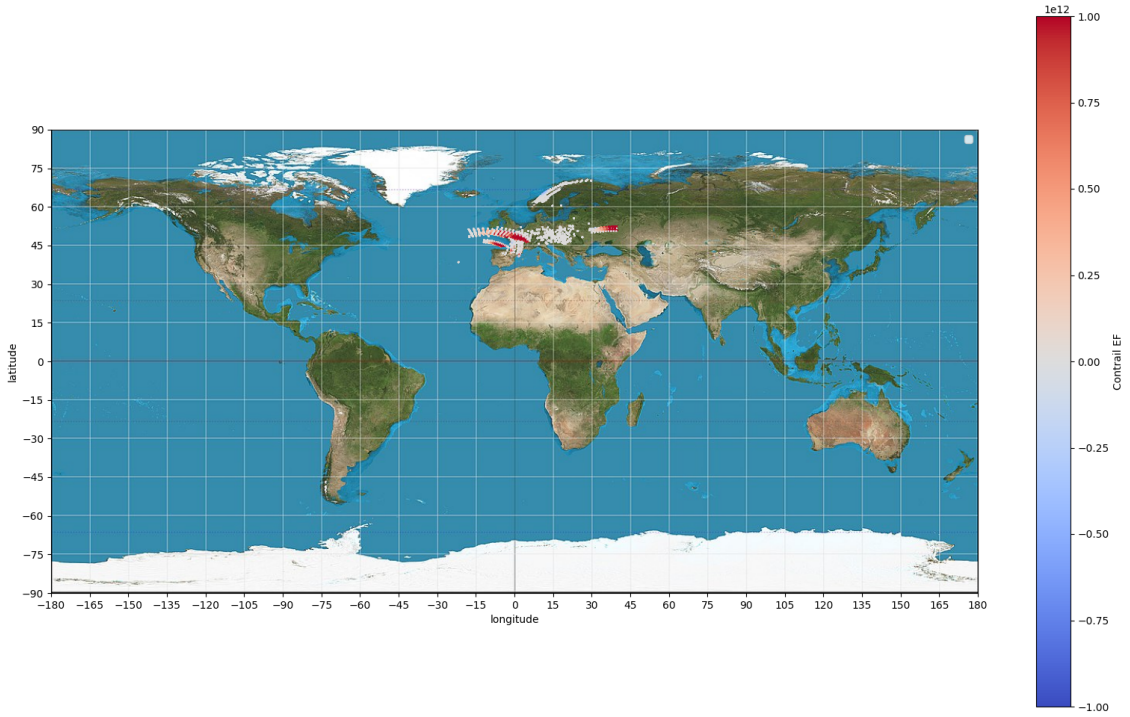

Figure 4.12: Contrails of flights starting and ending in Europe on the 8^{th} of March 2019

covered by these flights, their EF contribution remains relatively low. On average across all six days, intra-European flights account for only 11.03 % of the total EF.

Using the same methodology employed for transatlantic flights yields an average reduction of only 0.38 % in the total EF for the day, equivalent to 306.33 $1e^{12}$ J. Even the highest reduction observed on the 1^{st} of February, at 1.32 %, remains relatively low. The lowest reduction is recorded on the 29^{th} of April, amounting to only 5.3 $1e^{12}$ J, representing a mere 0.04 % of the total EF.

Table 4.5: Results for all days

Date	Timeslot		EF_{day} jet fuel [1e12 J]	EF_{day} SAF-blend [1e12 J]	Reduction [1e12 J]	Reduction [%]
100 % SAF						
Feb 01	16:12:00	17:24:00	89429.08	86632.78	2796.30	3.13
Mar 08	15:36:00	16:48:00	29315.65	26269.19	3046.46	10.39
Apr 29	11:24:00	12:36:00	14443.08	12367.98	2075.10	14.37
Jul 01	20:48:00	22:00:00	104491.82	99874.78	4617.04	4.42
Aug 13	19:24:00	20:36:00	11972.40	11489.78	482.62	4.03
Nov 15	09:36:00	10:48:00	210454.25	193009.97	17444.28	8.29
75 % SAF						
Feb 01	16:12:00	17:48:00	89429.08	86274.12	3154.96	3.53
Mar 08	15:36:00	16:48:00	29315.65	26269.19	3046.46	10.39
Apr 29	11:24:00	13:00:00	14443.08	12061.41	2381.67	16.49
Jul 01	20:48:00	22:24:00	104491.82	98840.40	5651.42	5.41
Aug 13	19:48:00	21:24:00	11972.40	11321.37	651.03	5.44
Nov 15	10:00:00	11:36:00	210454.25	190530.63	19923.62	9.47
50 % SAF						
Feb 01	14:48:00	17:12:00	89429.08	85306.81	4122.27	4.61
Mar 08	14:24:00	16:48:00	29315.65	25725.00	3590.65	12.25
Apr 29	11:24:00	13:48:00	14443.08	12033.30	2409.78	16.68
Jul 01	19:24:00	21:48:00	104491.82	97628.03	6863.79	6.57
Aug 13	19:12:00	21:48:00	11972.40	11110.83	861.57	7.20
Nov 15	09:24:00	11:48:00	210454.25	188518.31	21935.94	10.42
25 % SAF						
Feb 01	13:48:00	18:36:00	89429.08	88357.86	1071.22	1.20
Mar 08	12:00:00	16:48:00	29315.65	25839.81	3475.84	11.86
Apr 29	11:24:00	16:12:00	14443.08	12507.05	1936.03	13.40
Jul 01	17:36:00	22:24:00	104491.82	98087.98	6403.84	6.13
Aug 13	16:48:00	21:36:00	11972.40	11297.89	674.51	5.63
Nov 15	08:48:00	13:36:00	210454.25	185179.59	25274.66	12.01
5 % SAF						
Feb 01	24:00:00	00:00:00	89429.08	87104.41	2324.67	2.60
Mar 08	24:00:00	00:00:00	29315.65	28361.12	954.53	3.26
Apr 29	24:00:00	00:00:00	14443.08	13822.68	620.40	4.30
Jul 01	24:00:00	00:00:00	104491.82	101212.03	3279.79	3.14
Aug 13	24:00:00	00:00:00	11972.40	11739.80	232.60	1.94
Nov 15	24:00:00	00:00:00	210454.25	188899.10	21555.15	10.24

5
Discussion

5.1 Analysis of the 1^{st} of July 2019

Transitioning from detailed analysis to a broader perspective, the examination begins with a single day. Hence, the focus is on the 1^{st} of July, chosen due to the availability of original data. The findings are succinctly summarized in Table 5.1.

Table 5.1: Reduction over the whole day of different SAF-blends

SAF	EF whole day		Reduction		Contrail forming flights		Mean contrail age	
	Ref [1e12 J]	SAF [1e12 J]	Total [1e12 J]	Relative [%]	Ref [%]	SAF [%]	Ref [h]	SAF [h]
100 %	104491.82	99874.78	4617.04	4.42	16.97	19.97	6.02	5.56
75 %	104491.82	98840.40	5651.42	5.41	17.44	19.70	5.92	5.67
50 %	104491.82	97628.03	6863.79	6.57	15.48	16.84	4.71	4.64
25 %	104491.82	98087.98	6403.84	6.13	15.63	16.24	4.43	4.37
5 %	104491.82	101212.03	3279.79	3.14	8.14	8.22	5.26	5.23

It is evident that employing a blend of 50 % SAF and 50 % jet fuel yields the highest reduction at 6.57 %, equivalent to 6 863.73 $1e^{12}$ J. This is closely trailed by the blend of 25 % SAF and 75 % jet fuel, resulting in a reduction of 6.13 % or 6 403.84 $1e^{12}$ J. Conversely, using 75 % SAF leads to a reduction of only 5.41 %, while employing 100 % SAF results in a reduction of 4.42 %. Employing an even distribution with 5 % SAF over the entire day records an even lower reduction at only 3.14 %. The question arises: why do some distributions lead to a much higher reduction than others in SAF-blends?

Starting with the blend consisting of 5 % SAF and 95 % jet fuel, which exhibits the lowest reduction, the explanation can be found in the distribution of EF throughout the day in the reference case with only jet fuel (as depicted in Table 4.1). Some hours contribute to high EF, while others result in smaller or even negative EF. Negative EF cools the atmosphere, so using SAF during those hours would counterproductively reduce the cooling effect. Since the purpose of the SAF is to lower the warming effect, cooling contrails help to limit the warming effect. When the EF with jet fuel is already low, the potential for reducing the EF through SAF use diminishes. Therefore, distributing SAF evenly over the entire day yields less reduction than concentrating its use during specific hours with a higher EF.

Another aspect to consider is the percentage of flights contributing to contrail

formation. In the time blocks selected for other SAF-blends, contrails are formed by 15 to 20 % of flights. However, over the entire day, contrails are only formed by around 8 % of flights, whether using 5 % SAF or only jet fuel. This means that SAF is used in 7 to 12 % more flights that do not contribute to contrail formation, thereby limiting the potential reduction of EF. Given the variability of weather conditions and geographical locations, it is highly unlikely that a uniform use of 5 % SAF over the entire day would yield the best results.

The second lowest reduction, observed with 100 % SAF use in 1 hour and 12 minutes, can be attributed to opposing reasons. Whereas previously the time span for SAF use was too broad, here it is too narrow. Selecting the time with the highest EF naturally presents a high potential for reducing the EF, but this potential is limited by weather conditions. This means some contrails exhibit nearly similar climate effects whether fueled by 100 % SAF or jet fuel. Consequently, the use of SAF does not result automatically in a significant reduction in EF. Therefore, it is better to spread the amount of SAF over more flights.

This trend is evident in the distribution of 75 % SAF and 25 % jet fuel. The reduction increases from 4.42 % to 5.41 %, and further with 50 % SAF use, reaching 6.57 %. However, with 25 % SAF use over 4 hours and 48 minutes, the time span becomes too broad again to target the hours with the highest EF, as achieved with the 50 % SAF blend. Nevertheless, it still surpasses the reductions achieved with 100 % and 75 % use with 6.13 %. The reason for this lies in the fact that the 50 % use targets the precise hours of high EF, whereas spreading the SAF distribution lowers the average EF per flight, resulting in a less pronounced reduction. Despite this, it still outperforms the narrower time span approaches.

The increase in the number of flights producing contrails when using SAF is a noteworthy observation. With SAF as a fuel, the emission of water particles increases, leading to more flights forming contrails that previously did not. The higher the share of SAF, the greater the increase in the number of flights producing contrails. For instance, with 100 % SAF, there is a 3 % increase in contrail-producing flights, which decreases to 2.3 %, 1.4 %, 0.60 %, and finally only 0.06 % with 5 % SAF. This relationship is also related to the increasing number of flights in the analyzed time blocks. However, the underlying reason for the increase in contrail-forming flights with SAF compared to jet fuel remains consistent.

Conversely, higher SAF shares lead to a reduction in the mean contrail age. For example, with 100 % SAF, the mean contrail age is reduced by nearly 0.5 hours, while with 5 % SAF, it is shortened by only 0.03 hours, equivalent to less than 2 minutes. This reduction in contrail lifetime is attributed to the decreasing nvPM. As nvPM decreases, so does the contrail's lifetime. This observation aligns with findings by Teoh [4], where similar effects were observed and which were also mentioned in chapter 2.1.3.

Indeed, the analysis of the 1st of July highlights that spreading the use of SAF over a larger time span with lower SAF concentration yields more significant effects than using all of it at once in a small time block. However, spreading it too much over the day has even less effect than concentrating it in a very smaller time span. Therefore, the optimal strategy lies in using 25 % SAF or 50 % SAF, as indicated by the results of the analysis.

Moreover, the presence of different time zones in Europe adds complexity to selecting such a small time span for concentrated SAF use, as the hour on the clock changes along geographic lines while the changes in sunlight, which significantly influence EF, are continuous.

However, these conclusions are drawn from the analysis of only one day. To provide robust support for these findings, it is imperative to analyze the other modeled days to either corroborate or refute the assumptions made here. Evaluating multiple days will help ascertain if the observed trends are consistent across different meteorological conditions and flight patterns.

5.2 Different days

The ranking of SAF-blend effectiveness in reducing emissions can vary from one day to another (see Figure 4.7 or Figure 5.1). For instance, on most days, including the 1st of July, the 50 % SAF blend yields the greatest reduction, but this trend may not hold true on every day, such as the 15^{th} of November. On average, employing a 50 % blend of SAF and jet fuel results in a reduction of 9.62 % in the total emissions for the day. The rationale behind the efficacy of the 50 % blend has been discussed in previous sections. Therefore, it is pertinent to investigate why this blend does not exhibit the highest reduction on the 15^{th} of November.

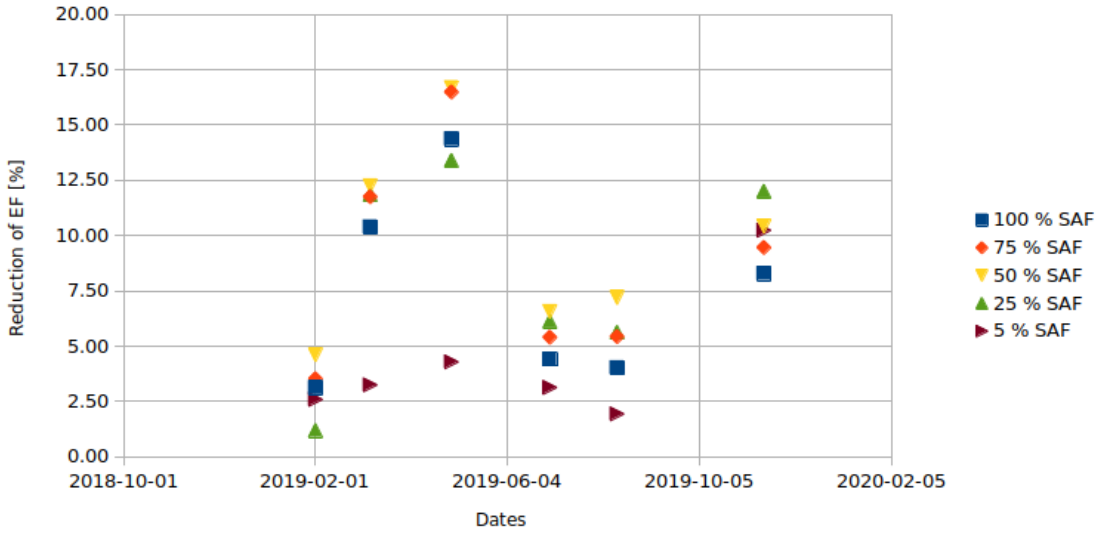

Figure 5.1: Reduction of EF each analyzed day in percentage

On the 15^{th} of November, the blend with the highest reduction is composed of 25 % SAF and 75 % jet fuel, resulting in a reduction of 12.01 %. Surprisingly, the 50 % blend only yields a reduction of 10.42 %. This discrepancy becomes clearer when examining the percentage of the total EF over two-hour blocks (see Figure 5.2).

The figure illustrates the distribution of the total EF over two-hour blocks throughout the day, with each day represented by a different color. For instance, the light blue line represents data from the 15^{th} of November, showing that aircraft departing

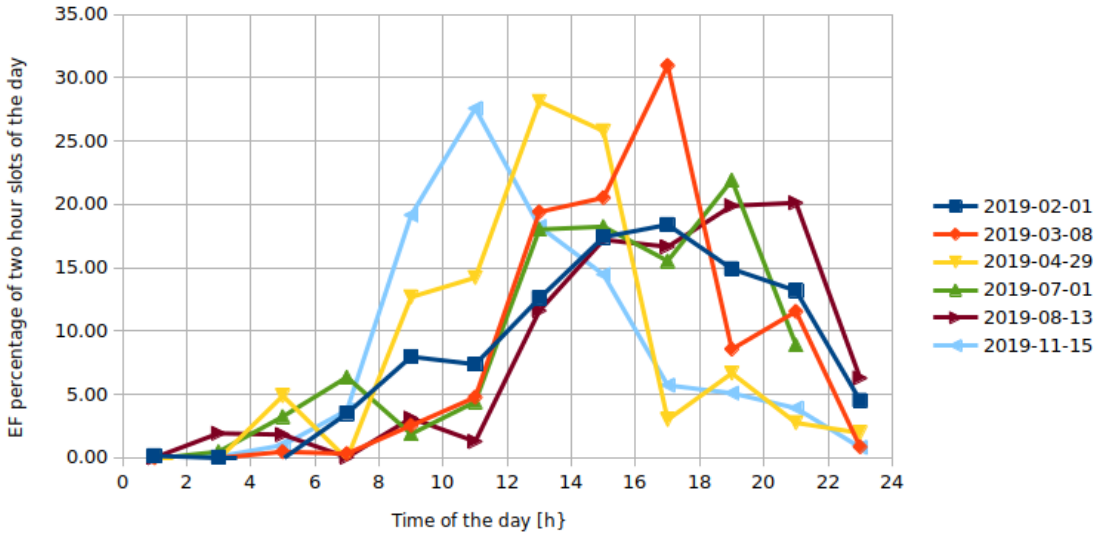

Figure 5.2: Share of EF from 2 hour blocks of the whole day

between 10 o'clock and 12 o'clock account for approximately 27.5 % of the total EF for that day. A higher share of the total EF indicates greater potential for reduction through the use of SAF, whereas a lower share implies less room for reduction.

Examining the data for the 15^{th} of November reveals that the day exhibits a peak between 10 and 12 o'clock, contributing to 27.5 % of the total EF. Additionally, the two-hour blocks before (19.15 %) and after (18.25 %) also show high values. Therefore, spreading the SAF more out, contributes to a higher reduction of EF then only using it a the peak. Conversely, on the 8^{th} of March, the three two-hour blocks with the highest share — 12 to 14 (19.4 %), 14 to 16 (20.53 %), and 16 to 18 (30.96 %)—are even higher than those on the 15^{th} of November. This might suggest that the 25 % blend should outperform the 50 % blend. However, this is not the case because the peak on the 8th of March is much smaller or "steeper" on the graph. Therefore, using 25 % SAF over a longer duration (4 hours and 48 minutes) leads to worse reduction than using 50 % SAF over a shorter period (2 hours and 24 minutes).

When the peak is steeper, the blend of 75 % SAF and 25 % jet fuel also demonstrates high reduction potential. This is evident on the 8^{th} of March and 29^{th} of April, where the steep peaks result in reductions of the total EF comparable to using a 50 % blend of SAF and jet fuel.

Another notable observation from Figure 5.2 is that on the 1^{st} of February, the blend with 25 % SAF exhibits the lowest reduction. Additionally, on the 8^{th} of March and 29^{th} of April, the 5 % SAF blend shows considerably lower reduction compared to other blends. Both of these points can be elucidated by examining the cumulative EF percentage over the hours (see Figure 5.3).

On the 1^{st} of February, there is a relatively consistent gradient over several time blocks, along with the lowest maximum gradient of all the days studied. This suggests that on this particular day, contrails with a significant impact on the EF are more evenly spread throughout the day compared to other days. Consequently,

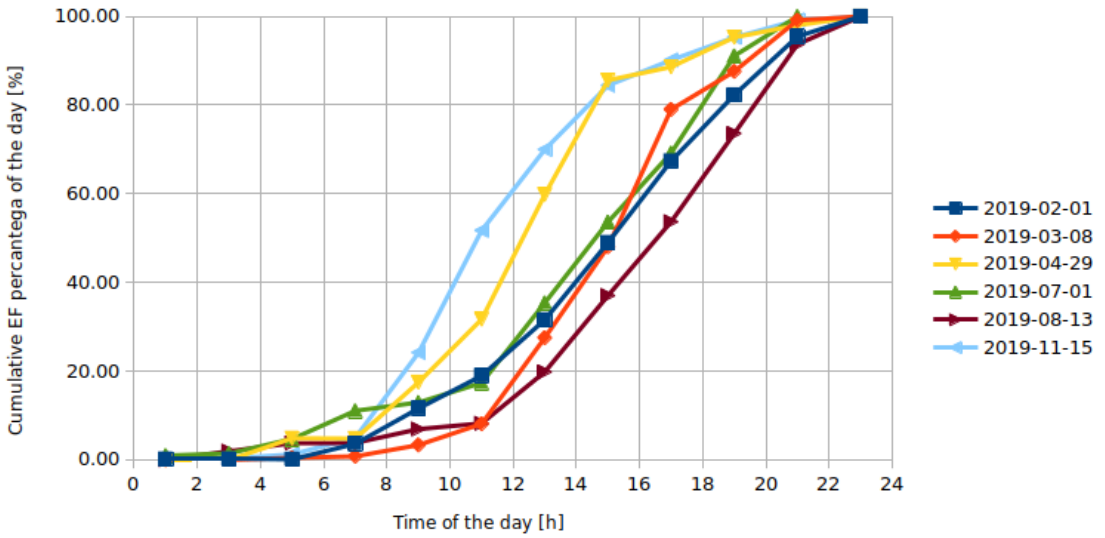

Figure 5.3: Cumulative percentage EF of the day

there is not a higher EF over extended periods, resulting in a higher reduction when using a 5 % SAF blend over the entire day compared to a 25 % blend over 4 hours and 48 minutes. However, even with the relatively low maximum gradient, the 50 %, 75 %, and 100 % SAF blends still bring about higher reductions than the 5 % blend.

The very low reduction observed with the 5 % blend on the 8^{th} of March and 29^{th} of April can also be explained by their high maximum gradients, or the peaks in the distribution (Figure 5.2). This indicates that at certain points during these days, the EF is notably high, making it more effective to use a higher proportion of SAF in a shorter time span.

In summary, the highest reduction can be achieved with a blend of 50 % SAF and 50 % jet fuel, resulting in an average reduction of 9.62 % of the EF compared to using only jet fuel type A throughout the day. The second-best options are blends of 75 % SAF and 25 % jet fuel or vice versa, which yield reductions of 8.68 % and 8.37 % respectively compared to using only jet fuel. However, it is important to note that reduction is highly dependent on meteorological conditions, as evidenced by the significant variation between days. For example, the total EF on the 15^{th} of November is approximately 17 times higher than on the 13^{th} of August.

Meteorological conditions also strongly influence the timing of the day with the highest EF, which should be considered when selecting the appropriate SAF blends. Based on the analysis of six days, it can be generally recommended to use SAF blends during peak hours, which typically occur between 10 o'clock and 20 o'clock. However, this recommendation can be further refined based on the season. For instance, in spring, a 50 % SAF blend between 12 and 18 o'clock is suggested, as this aligns with the peak hours observed in March and April. In summer, particularly July and August, SAF should be utilized in the evening, between 18 and 22 o'clock, when the peak occurs. Conversely, in fall (November), using SAF during morning hours (between 10 and 12 o'clock) aligns with the observed peak. Finally, in winter (February), although there is not a distinct peak, utilizing SAF between 14 and 20

o'clock coincides with the highest points observed.

For more precise time selection, further analysis of additional days is recommended. Ultimately, weather forecasts should be consulted to predict the optimal starting time for flights with the highest EF.

5.3 Flights from Europe to North America

As mentioned in Chapter 4.4, flights from Europe to North America contribute significantly to the total EF for the entire day. On average, these flights are responsible for 47.36 % of the total EF, despite accounting for only 16.94 % of the distance of the flights originating in Europe. This disproportionate impact can be attributed to several factors. Firstly, flights to North America typically reach high altitudes, where lower temperatures and reduced air density favor contrail formation. Therefore, they more often fulfill the SAC. Additionally, the extended duration of these flights increases the likelihood of contrail formation and encounter ice supersaturated areas. Furthermore, the warming effect of contrails is most pronounced when they form over dark surfaces, such as the sea, which is often the case for flights over the North Atlantic (as discussed in Chapter 2.1.2).

The significant contribution of these flights to the total EF underscores the potential for EF reduction through the use of SAF. However, it is important to note that both the initial EF generated by conventional jet fuel and the subsequent reduction achieved by SAF are heavily influenced by weather conditions. This variability is evident in the differences observed in reduction percentages across the analyzed days (see Figure 5.4).

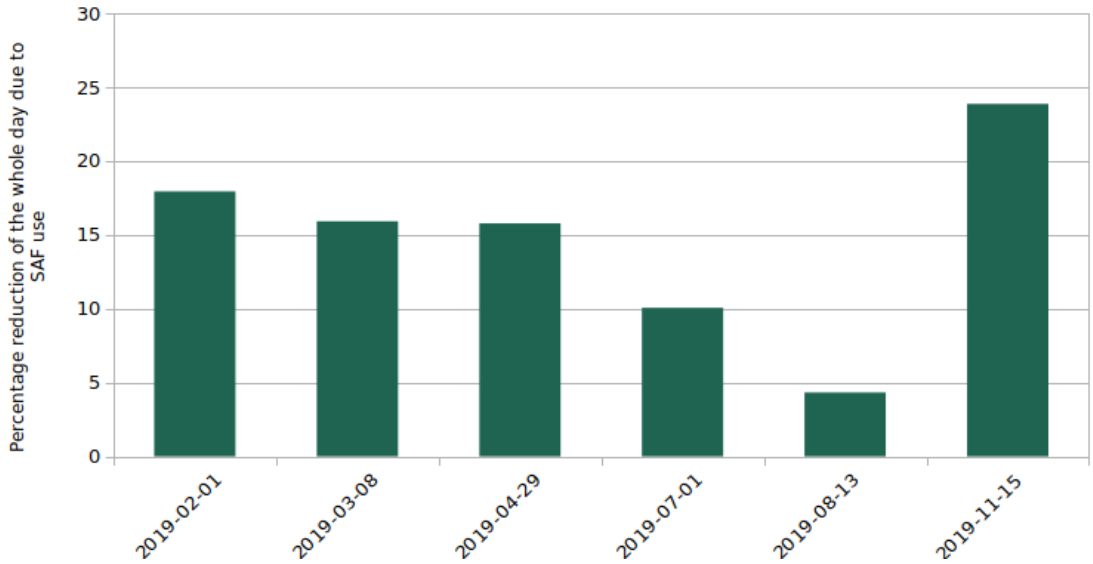

Figure 5.4: Reduction on each day for flights from Europe to North America due to SAF use

On the 13^{th} of August, the share of EF attributable to flights from Europe to North America was approximately 10 %, resulting in a reduction of under 5 % due to the use of SAFs. In contrast, the 15^{th} of November stands out with a reduction of nearly

25 %. This notable difference can be attributed to favorable weather conditions for SAF use on that day. Similarly, on the 1^{st} of February, meteorological conditions were conducive to contrail reduction, resulting in the second-highest reduction of 17.95 %, despite the flight's share of EF being only 33 %.

As previously discussed, when comparing the proportion of flown kilometers to the share of EF and subsequent EF reduction, it becomes evident that using SAF in these flights leads to a significant reduction in EF.

5.4 Inter european flights

As highlighted in the results, the discrepancy between the share of flown distance and the share of EF is significant. This is primarily due to the nature of flights within Europe, where aircraft typically operate at lower altitudes for shorter durations. Consequently, the overall EF generated by these flights is relatively low.

Furthermore, contrail formation occurs only among a small fraction of flights. For instance, on the 15^{th} of November, only 4.56 % of flights using jet fuel were responsible for contrail formation, a figure that marginally increased to 4.68 % with the use of SAF. This implies that over 95 % of the SAF usage in these flights does not contribute to contrail reduction, as the majority of flights do not generate contrails. Consequently, the utilization of SAF in inter-European flights does not significantly reduce contrail-related EF.

5.5 Comparing the different approaches

After presenting and deliberating on the outcomes of each approach individually, it becomes imperative to compare them with one another. The primary focus for comparison lies in the EF and the subsequent reduction achieved through the use of SAF. The most dependable metric for comparison is the average reduction percentage across all days relative to the total EF for those days. This approach is necessary due to the substantial variations in EF observed across different days.

The approach yielding the highest average reduction is the utilization of SAF in flights from Europe to North America, with a blend comprising 29.51 % SAF and 70.49 % jet fuel. This results in a reduction of 14.65 % compared to the reference day when only jet fuel is employed.

Following closely is the use of a 50/50 blend of SAF and jet fuel over a duration of 2 hours and 24 minutes during the period of highest EF of the day, achieving an average reduction of 9.62 %. This is succeeded by blends of 75 % SAF and 25 % jet fuel, yielding an average reduction of 8.68 % and 25 % SAF with 8.37 % reduction on average. Subsequently, employing 100 % SAF over a duration of only 1 hour and 12 minutes results in a reduction of 7.44 %. Surprisingly, even distributing 5 % SAF evenly over the entire day for all flights leads to a larger reduction of 4.25 % compared to using SAF exclusively for inter-European flights, which achieves an average reduction of only 0.38 % when employing a blend of 9.63 % SAF and 90.37 % jet fuel.

The rationale behind the ordering of these approaches has been previously discussed in earlier chapters. Additionally, it should be noted that within the selected time slots for each approach, a significant portion of contrails with high EF impact are formed over the North Atlantic or North America. This underscores the substantial influence these flights have on the overall EF.

Moreover, implementing a strategy to fuel all flights bound for North America with the same SAF and jet fuel blend at the time of departure, coinciding with the period of highest EF generation, is considerably more feasible. However, pinpointing the ideal time slot can be challenging due to weather-dependent variations. While retrospective analysis of flight paths can provide insights into optimal timing, predicting peak EF hours using weather forecasts poses a significant challenge. Therefore, applying SAF to flights destined for North America emerges as a more sensible approach.

Indeed, the implementation of SAFs consistently leads to a reduction in EF across all cases. This can be attributed to the reduction in nvPM resulting from the use of SAFs. As a result, contrails have a shorter lifetime, thereby mitigating their climate impact. Moreover, the optical depth of these contrails is reduced due to the decreased presence of nvPM. Additionally, SAFs significantly reduce CO_2 emissions, making them a viable substitute for conventional jet fuel in all scenarios.

The reduction of CO_2 was not explicitly investigated in this thesis but is well-documented in the literature, such as in the work by Teoh [4]. Teoh's studies ([4], [10], [13], [7]) present results that align closely with the findings of this thesis. Specifically, Teoh demonstrates that the nvPM decreases with a higher share of SAF, a logical outcome given that his formula was employed in the calculations in this thesis. Furthermore, numerous other similarities are observed. For instance, the proportion of flights producing contrails increases as the share of SAF rises. Additionally, the age of contrails decreases with higher SAF content. Notably, Teoh's research indicates that the EF is reduced by nearly 50 % when comparing the baseline scenario with the use of 100 % SAF for flights over the North Atlantic [4]. These findings are consistent with the results of this thesis and suggest that similar reductions in CO_2 emissions, as reported by Teoh, can be inferred here due to the numerous similarities. Of course, the amount of SAF needs to be comparable, which would be approximately SAF30, as the flights from Europe to North America used a SAF-blend of 29.51 %.

Furthermore, Teoh's article „Understanding the role of contrails „[4] provides valuable insights into the daily variations in net RF, particularly for flights over the North Atlantic (Figure 2). Although this analysis is specific to North Atlantic flights, it is highly relevant due to the significant contribution of these flights to overall RF respectively EF. Teoh's findings on the daily and seasonal shifts in hours of peak RF reinforce the conclusions drawn in this thesis regarding the optimal times of day for the maximum EF.

6
Conclusion

The objective of this research was to establish a rule of thumb for mitigating the climate impact of contrails through the use of SAFs. The initial premise was to allocate a fixed share of 5 % SAF across all flights originating from Europe throughout the day. Through various analyses, it was determined that the optimal approach is to allocate all SAF to flights originating in Europe and bound for North America. This resulted in a notable reduction of 14.65 % in total EF when employing the highest possible blend of 29.51 % SAF.

Conversely, the least effective use of SAFs, as indicated by the analyses, is their allocation solely to inter-European flights. While this scenario is the most probable due to incentives for CO_2 reductions typically being tied to intra-European flights, the impact on EF reduction is minimal, averaging only 0.38 %.

Another approach examined was the timing of SAF use during the day. The highest reduction of 9.62 % was achieved by employing a blend of 50 % SAF and 50 % jet fuel during a 2-hour and 24-minute window coinciding with the peak EF period. Variations in the blend percentages (100 %, 75 %, and 25 %) necessitated different durations to maintain the 5 % SAF ratio. Additionally, an even distribution of 5 % SAF throughout the day yielded lower reductions compared to other blends but still outperformed exclusive use in inter-European flights.

The optimal time slot for SAF utilization varied from day to day, heavily influenced by meteorological conditions. While weather forecasting could aid in selecting ideal time slots, perfect predictions remain elusive. As a general guideline, springtime warrants SAF use between 12:00 and 18:00, while summer favors usage from 18:00 to 22:00, autumn from 10:00 to 12:00, and winter from 14:00 to 20:00.

However, this rule of thumb is based on a limited analysis of six days. Further investigation with more data is warranted, considering the strong weather dependency of EF. Nevertheless, prioritizing SAF use in flights to North America remains the most sensible approach.

As the demand for SAF increases in the future to bolster CO_2 mitigation efforts, it is imperative to allocate these resources primarily to long-distance flights. Additionally, conducting research on all flights departing from Europe, as they are likely to have a significant EF impact, could further inform SAF allocation strategies. Ultimately, prioritizing SAF use in flights with the highest EF impact maximizes potential reductions and contributes to more effective climate mitigation efforts.

Bibliography

[1] Deutscher Wetterdienst. "2023 ist wärmstes Jahr seit Messbeginn". In: (2023). URL: https://www.tagesschau.de/wissen/klima/wetter-jahresbilanz-dwd-100.html.

[2] Bundesministerium für Umwelt, Naturschutz, Bau und Reaktorsicherheit (BMUB), www.bmub.bund.de. "Übereinkommen von Paris". In: (2015). URL: https://www.bmz.de/de/service/lexikon/klimaabkommen-von-paris-14602.

[3] Susanne Pettersson. *Analyzing the climate impacts of sustainable aviation fuels*. Gothenburg, 2023. URL: https://annonsportal.chalmers.se/CareerServices/en/Ads/Details/2064.

[4] Roger Teoh et al. "Targeted Use of Sustainable Aviation Fuel to Maximize Climate Benefits". In: *Environmental science & technology* 56.23 (2022), pp. 17246–17255. DOI: 10.1021/acs.est.2c05781.

[5] Dharmendra Kumar Singh, Swarnali Sanyal, and Donald J. Wuebbles. *Understanding the Role of Contrails and Contrail Cirrus in Climate Change: A Global Perspective*. 2024. DOI: 10.5194/egusphere-2024-127.

[6] European Union Aviation Safety Agency. *Current landscape and future of SAF industry*. 2020. URL: https://www.easa.europa.eu/eco/eaer/topics/sustainable-aviation-fuels/current-landscape-future-saf-industry#production-capacity-and-demand-beyond-2030-to-2050.

[7] R. Teoh et al. "The high-resolution Global Aviation emissions Inventory based on ADS-B (GAIA) for 2019–2021". In: 24.1 (2024), pp. 725–744. DOI: 10.5194/acp-24-725-2024. URL: https://acp.copernicus.org/articles/24/725/2024/.

[8] U. Schumann. "A contrail cirrus prediction model". In: *Geoscientific Model Development* 5.3 (2012), pp. 543–580. DOI: 10.5194/gmd-5-543-2012.

[9] Bernd Kärcher. "Formation and radiative forcing of contrail cirrus". In: *Nature communications* 9.1 (2018), p. 1824. DOI: 10.1038/s41467-018-04068-0.

[10] Roger Teoh. *Aircraft contrail climate effects and mitigation*. Online, 2/03/2022. URL: https://www.youtube.com/watch?v=AxnB1aWggUc&t=127s.

[11] Inés Sanz-Morère et al. "Reducing Uncertainty in Contrail Radiative Forcing Resulting from Uncertainty in Ice Crystal Properties". In: *Environmental Science & Technology Letters* 7.6 (2020), pp. 371–375. DOI: 10.1021/acs.estlett.0c00150.

[12] Lisa Bock and Ulrike Burkhardt. "Reassessing properties and radiative forcing of contrail cirrus using a climate model". In: *Journal of Geophysical Research: Atmospheres* 121.16 (2016), pp. 9717–9736. DOI: 10.1002/2016JD025112.

[13] Roger Teoh et al. *Aviation contrail climate effects in the North Atlantic from 2016–2021*. 2022. DOI: 10.5194/acp-2022-169.

[14] D. S. Lee et al. "The contribution of global aviation to anthropogenic climate forcing for 2000 to 2018". In: *Atmospheric environment (Oxford, England : 1994)* 244 (2021), p. 117834. ISSN: 1352-2310. DOI: 10.1016/j.atmosenv.2020.117834.

[15] Christiane Voigt et al. "Cleaner burning aviation fuels can reduce contrail cloudiness". In: *Communications Earth & Environment* 2.1 (2021). DOI: 10.1038/s43247-021-00174-y.

[16] Stefanie Waldek. *Contrails: What are they and how do they form?* space.com, 2023. URL: https://www.space.com/what-are-contrails#section-additional-resources.

[17] Richard McCausland. "Net zero 2050: sustainable aviation fuels". In: (2023). URL: https://www.iata.org/en/programs/environment/sustainable-aviation-fuels/.

[18] Ulrich Schumann. "A contrail cirrus prediction tool". In: (2009).

[19] Marc Shapiro et al. *pycontrails: Python library for modeling aviation climate impacts*. 2023. DOI: 10.5281/zenodo.10182539.

[20] Benjamin T. Brem et al. "Effects of Fuel Aromatic Content on Nonvolatile Particulate Emissions of an In-Production Aircraft Gas Turbine". In: *Environmental science & technology* 49.22 (2015), pp. 13149–13157. DOI: 10.1021/acs.est.5b04167.

[21] European Union. *system for greenhouse gas emission allowance trading within the Union*. URL: https://eur-lex.europa.eu/legal-content/EN/TXT/?uri=CELEX%3A02003L0087-20240301.

A

Appendix 1

Table A.1: European countries and their two letter country code

Code	Country
AD	Andorra
AL	Albania
AT	Austria
BA	Bosnia a. Herzegovina
BE	Belgium
BG	Bulgaria
BY	Belarus
CH	Switzerland
CZ	Czech Republic
DE	Germany
DK	Denmark
EE	Estonia
ES	Spain
FI	Finland
FR	France
GB	United Kingdom
GR	Greece
HR	Croatia
HU	Hungary
IE	Ireland
IS	Iceland
IT	Italy
LI	Liechtenstein
LT	Lithuania
LU	Luxembourg
LV	Latvia
MC	Monaco
MD	Moldova
ME	Montenegro
MK	North Macedonia
MT	Malta
NL	Netherlands
NO	Norway
PL	Poland
PT	Portugal
RO	Romania
RS	Serbia
SE	Sweden
SI	Slovenia
SK	Slovakia
SM	San Marino
VA	Vatican City

Table A.2: European countries and their two letter country code

Code	Country
AG	Antigua a. Barbuda
BB	Barbados
BM	Bermuda
BQ	Caribbean Netherlands
BS	Bahamas
BZ	Belize
CA	Canada
CR	Costa Rica
CU	Cuba
CW	Curaçao
DM	Dominica
DO	Dominican Republic
GD	Grenada
GL	Greenland
GP	Guadeloupe
GT	Guatemala
HN	Honduras
HT	Haiti
JM	Jamaica
KN	Saint Kitts a. Nevis
KY	Cayman Islands
LC	Saint Lucia
MQ	Martinique
MX	Mexico
NI	Nicaragua
PA	Panama
PM	Saint Pierre a. Miquelon
PR	Puerto Rico
SV	El Salvador
SX	Sint Maarten
TC	Turks a. Caicos Islands
TT	Trinidad a. Tobago
US	United States
VI	U.S. Virgin Islands

Table A.3: 12 minute time blocks and EF of the total contrails in the block

Time	**EF** [1e12 J]
13:36 - 13:48	757.57
13:48 - 14:00	-462.02
14:00 - 14:12	154.95
14:12 - 14:24	3828.10
14:24 - 14:36	984.11
14:36 - 14:48	483.75
14:48 - 15:00	2845.29
15:00 - 15:12	2255.30
15:12 - 15:24	1895.48
15:24 - 15:36	1753.18
15:36 - 15:48	1796.93
15:48 - 16:00	2841.40
16:00 - 16:12	805.68
16:12 - 16:24	1595.61
16:24 - 16:36	3781.14
16:36 - 16:48	2068.20
16:48 - 17:00	2094.98
17:00 - 17:12	2632.17
17:12 - 17:24	2008.07
17:24 - 17:36	457.29
17:36 - 17:48	2348.50
17:48 - 18:00	1276.94
18:00 - 18:12	1292.72
18:12 - 18:24	792.67
18:24 - 18:36	1848.43
18:36 - 18:48	1507.38
18:48 - 19:00	2460.94
19:00 - 19:12	961.45
19:12 - 19:24	572.43
19:24 - 19:36	2182.80
19:36 - 19:48	2520.57
19:48 - 20:00	2098.40
20:00 - 20:12	1100.21
20:12 - 20:24	1874.97
20:24 - 20:36	2151.84
20:36 - 20:48	572.69
20:48 - 21:00	3453.46
21:00 - 21:12	3525.26
21:12 - 21:24	3656.78
21:24 - 21:36	2120.09
21:36 - 21:48	3166.05
21:48 - 22:00	1284.81
22:00 - 22:12	2271.69
22:12 - 22:24	2952.13
22:24 - 22:36	452.08
22:36 - 22:48	923.42
22:48 - 23:00	271.79
23:00 - 23:12	36.17
23:12 - 23:24	410.07

Table A.4: 1 hour 12 minutes time blocks with a 1 hour overlay and the total EF of the contrails in the block

Time	**EF** [1e12 J]
13:36 - 14:48	5746.46
13:48 - 15:00	7834.18
14:00 - 15:12	10551.5
14:12 - 15:24	12292.03
14:24 - 15:36	10217.11
14:36 - 15:48	11029.93
14:48 - 16:00	13387.58
15:00 - 16:12	11347.97
15:12 - 16:24	10688.28
15:24 - 16:36	12573.94
15:36 - 16:48	12888.96
15:48 - 17:00	13187.01
16:00 - 17:12	12977.78
16:12 - 17:24	14180.17
16:24 - 17:36	13041.85
16:36 - 17:48	11609.21
16:48 - 18:00	10817.95
17:00 - 18:12	10015.69
17:12 - 18:24	8176.19
17:24 - 18:36	8016.55
17:36 - 18:48	9066.64
17:48 - 19:00	9179.08
18:00 - 19:12	8863.59
18:12 - 19:24	8143.3
18:24 - 19:36	9533.43
18:36 - 19:48	10205.57
18:48 - 20:00	10796.59
19:00 - 20:12	9435.86
19:12 - 20:24	10349.38
19:24 - 20:36	11928.79
19:36 - 20:48	10318.68
19:48 - 21:00	11251.57
20:00 - 21:12	12678.43
20:12 - 21:24	15235.00
20:24 - 21:36	15480.12
20:36 - 21:48	16494.33
20:48 - 22:00	17206.45
21:00 - 22:12	16024.68
21:12 - 22:24	15451.55
21:24 - 22:36	12246.85
21:36 - 22:48	11050.18
21:48 - 23:00	8155.92
22:00 - 23:12	6907.28
22:12 - 23:24	5045.66

Table A.5: 1 hour 36 minutes time blocks with an 1 hour and 24 minutes overlay and the total EF of the contrails in the block

Time	**EF** [1e12 J]
01:36:00 PM - 03:12:00 PM	10847.05
01:48:00 PM - 03:24:00 PM	11984.96
02:00:00 PM - 03:36:00 PM	14200.16
02:12:00 PM - 03:48:00 PM	15842.14
02:24:00 PM - 04:00:00 PM	14855.44
02:36:00 PM - 04:12:00 PM	14677.01
02:48:00 PM - 04:24:00 PM	15788.87
03:00:00 PM - 04:36:00 PM	16724.72
03:12:00 PM - 04:48:00 PM	16537.62
03:24:00 PM - 05:00:00 PM	16737.12
03:36:00 PM - 05:12:00 PM	17616.11
03:48:00 PM - 05:24:00 PM	17827.25
04:00:00 PM - 05:36:00 PM	15443.14
04:12:00 PM - 05:48:00 PM	16985.96
04:24:00 PM - 06:00:00 PM	16667.29
04:36:00 PM - 06:12:00 PM	14178.87
04:48:00 PM - 06:24:00 PM	12903.34
05:00:00 PM - 06:36:00 PM	12656.79
05:12:00 PM - 06:48:00 PM	11532
05:24:00 PM - 07:00:00 PM	11984.87
05:36:00 PM - 07:12:00 PM	12489.03
05:48:00 PM - 07:24:00 PM	10712.96
06:00:00 PM - 07:36:00 PM	11618.82
06:12:00 PM - 07:48:00 PM	12846.67
06:24:00 PM - 08:00:00 PM	14152.4
06:36:00 PM - 08:12:00 PM	13404.18
06:48:00 PM - 08:24:00 PM	13771.77
7:00:00 PM - 8:36:00 PM	13462.67
7:12:00 PM - 8:48:00 PM	13073.91
7:24:00 PM - 9:00:00 PM	15954.94
7:36:00 PM - 9:12:00 PM	17297.4
7:48:00 PM - 9:24:00 PM	18433.61
8:00:00 PM - 9:36:00 PM	18455.3
8:12:00 PM - 9:48:00 PM	20521.14
8:24:00 PM - 10:00:00 PM	19930.98
8:36:00 PM - 10:12:00 PM	20050.83
8:48:00 PM - 10:24:00 PM	22430.27
9:00:00 PM - 10:36:00 PM	19428.89
9:12:00 PM - 10:48:00 PM	16827.05
9:24:00 PM - 11:00:00 PM	13442.06
9:36:00 PM - 11:12:00 PM	11358.14
9:48:00 PM - 11:24:00 PM	8602.16

Table A.6: 2 hour 24 minutes time blocks with an 2 hours and 12 minutes overlay and the total EF of the contrails in the block

Time	**EF** [1e12 J]
01:36:00 PM - 04:00:00 PM	19134.04
01:48:00 PM - 04:12:00 PM	19182.15
02:00:00 PM - 04:24:00 PM	21239.78
02:12:00 PM - 04:36:00 PM	24865.97
02:24:00 PM - 04:48:00 PM	23106.07
02:36:00 PM - 05:00:00 PM	24216.94
02:48:00 PM - 05:12:00 PM	26365.36
03:00:00 PM - 05:24:00 PM	25528.14
03:12:00 PM - 05:36:00 PM	23730.13
03:24:00 PM - 05:48:00 PM	24183.15
03:36:00 PM - 06:00:00 PM	23706.91
03:48:00 PM - 06:12:00 PM	23202.7
04:00:00 PM - 06:24:00 PM	21153.97
04:12:00 PM - 06:36:00 PM	22196.72
04:24:00 PM - 06:48:00 PM	22108.49
04:36:00 PM - 07:00:00 PM	20788.29
04:48:00 PM - 07:12:00 PM	19681.54
05:00:00 PM - 07:24:00 PM	18158.99
05:12:00 PM - 07:36:00 PM	17709.62
05:24:00 PM - 07:48:00 PM	18222.12
05:36:00 PM - 08:00:00 PM	19863.23
05:48:00 PM - 08:12:00 PM	18614.94
06:00:00 PM - 08:24:00 PM	19212.97
06:12:00 PM - 08:36:00 PM	20072.09
06:24:00 PM - 08:48:00 PM	19852.11
06:36:00 PM - 09:00:00 PM	21457.14
06:48:00 PM - 09:12:00 PM	23475.02
07:00:00 PM - 09:24:00 PM	24670.86
07:12:00 PM - 09:36:00 PM	25829.50
07:24:00 PM - 09:48:00 PM	28423.12
07:36:00 PM - 10:00:00 PM	27525.13
07:48:00 PM - 10:12:00 PM	27276.25
08:00:00 PM - 10:24:00 PM	28129.98
08:12:00 PM - 10:36:00 PM	27481.85
08:24:00 PM - 10:48:00 PM	26530.30
08:36:00 PM - 11:00:00 PM	24650.25
08:48:00 PM - 11:12:00 PM	24113.73
09:00:00 PM - 11:24:00 PM	21070.34

Table A.7: 4 hour 48 minutes time blocks with an 4 hour and 36 minutes overlay and the total EF of the contrails in the block

Time	**EF** [1e12 J]
01:36:00 PM - 06:24:00 PM	40288.01
01:48:00 PM - 06:36:00 PM	41378.87
02:00:00 PM - 06:48:00 PM	43348.27
02:12:00 PM - 07:00:00 PM	45654.26
02:24:00 PM - 07:12:00 PM	42787.61
02:36:00 PM - 07:24:00 PM	42375.93
02:48:00 PM - 07:36:00 PM	44074.98
03:00:00 PM - 07:48:00 PM	43750.26
03:12:00 PM - 08:00:00 PM	43593.36
03:24:00 PM - 08:12:00 PM	42798.09
03:36:00 PM - 08:24:00 PM	42919.88
03:48:00 PM - 08:36:00 PM	43274.79
04:00:00 PM - 08:48:00 PM	41006.08
04:12:00 PM - 09:00:00 PM	43653.86
04:24:00 PM - 09:12:00 PM	45583.51
04:36:00 PM - 09:24:00 PM	45459.15
04:48:00 PM - 09:36:00 PM	45511.04
05:00:00 PM - 09:48:00 PM	46582.11
05:12:00 PM - 10:00:00 PM	45234.75
05:24:00 PM - 10:12:00 PM	45498.37
05:36:00 PM - 10:24:00 PM	47993.21
05:48:00 PM - 10:36:00 PM	46096.79
06:00:00 PM - 10:48:00 PM	45743.27
06:12:00 PM - 11:00:00 PM	44722.34
06:24:00 PM - 11:12:00 PM	43965.84
06:36:00 PM - 11:24:00 PM	42527.48

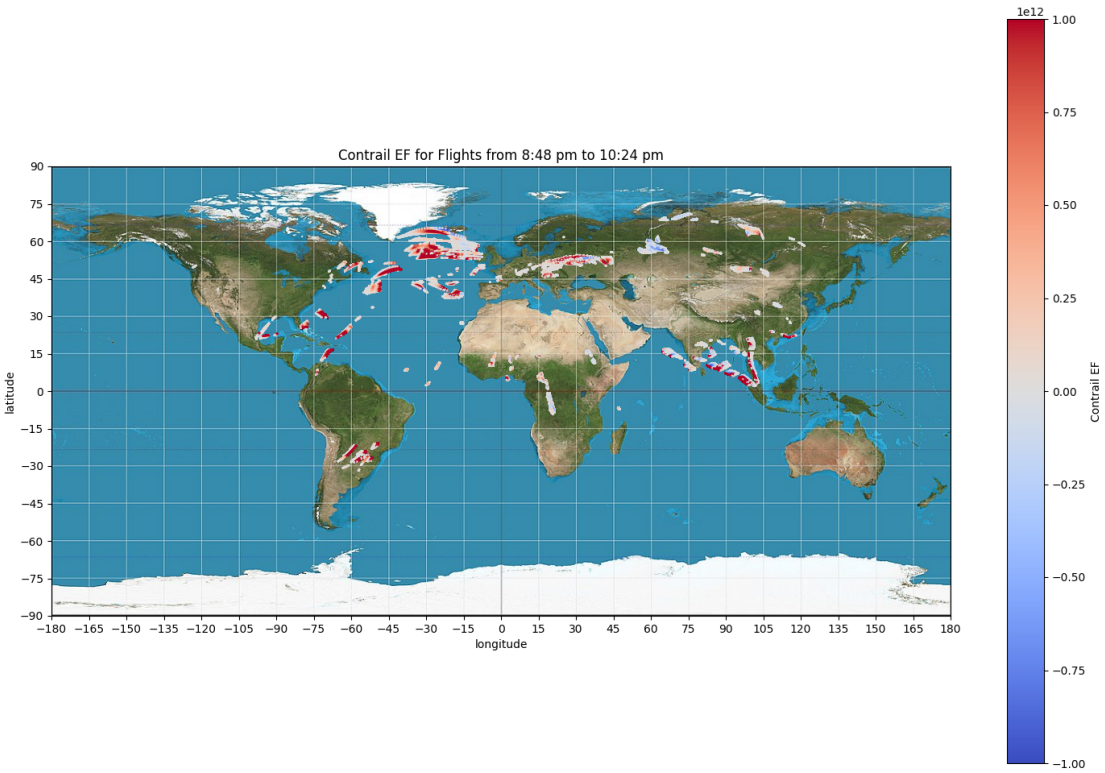

Figure A.1: EF of contrails due to flights with starting time between 8:48 pm and 10:24 pm on the 1^{st} of July 2019 with starting point in Europe; Fuel: 100% SAF

DEPARTMENT OF SOME SUBJECT OR TECHNOLOGY
CHALMERS UNIVERSITY OF TECHNOLOGY
Gothenburg, Sweden
www.chalmers.se

CHALMERS
UNIVERSITY OF TECHNOLOGY